Physics Beyond Standard Model

- Standard Model
- Neutrino Search
- Big Bang Dark Matter
- Big Bang Dark Energy
- Quantum entanglement（量子纠缠）

J. Ulbricht ETHZ Lecture USTC 2017

OUTLINE

- History of Big Bang and Dark matter observations
- Transition SM to Big Bang
- PARAMETERS of Lambda-CDM model
- Evolution of the COSMOS
- The parameters of the ΛCDM model get restricted by 8 observations
- Experimental search for Dark Matter
- Conclusion

History of Big Bang and Dark matter observations

- 1908 Walter S. Adams use first the “term red-shift”.
- 1912 Vesto Sliper discovered most spiral nebula had red shift.
- 1922 E. Hubbel and a. Friedman introduced the Hubble law and the Friedman equations.
- 1932 Jian Oort studied stellar motions in neighbourhood galaxies and found that the mass on the galactic plane must be more as the visible mass.
- 1933 Fritz Zwicky studied the stability of the COMA cluster and found evidence of unseen mass. He inferred that a non-visible mass must exist which provides enough mass and gravity to hold the cluster together.
- 1948 R. Alpher and R. Herman predicted the Micro Wave background.
- 1978 A. Penzieas and R. W. Wilson got Nobel Price for discovery of 2.7 K Micro Wave background.
- 1960 – 1980 The observations and calculations of Vera Rubin and Kent Ford showed that most galaxies must contain about ten times more mass as can be accounted for visible stars to explain the galactic rotation curves.
- 1997 The DAMA experiment in Gand Sasso reported about an annual modulation signature over many annual cycles.
- 2012 Lensing observations identify a filament of dark matter between two clusters of galaxies.
- 2013 First high energy events from IceCupe Neutrino Observation

Transition SM to Big Bang

To compare the SM and Big Bang model it is necessary to discuss the ***fours dimension*** the time.

$$(x_2, y_2, z_2, t_2)$$

SM - Theory

Big Bang

Action Integral S

Line element $\boxed{ds^2}$

$$(x_1, y_1, z_1, t_1)$$

$$\boxed{S = f(x, y, z, t; SM - parameters)}$$

$$\boxed{ds^2 = f(x, y, z, t; Big - Bang - parameters)}$$

$$\boxed{S = f(x,y,z,t;SM-parameters)}$$

$$\boxed{ds^2 = f(x,y,z,t;Big-Bang-parameters)}$$

Action Integral S

$$S = \int_{t_1}^{t_2} L\,dt$$

INVARIANC — CONSERVATION

time → energy

space → momentum

rotation → angular momentum

$$\mathcal{S} = \int \bar{\psi}(i\hbar c\gamma^\mu\partial_\mu - mc^2)\psi\,\mathrm{d}^4x$$

Global gauge $\psi(x) \to \psi'(x) = e^{i\xi}\psi(x)$

Current conservation

Local gauge $\psi(x) \to \psi'(x) = e^{i\xi(x)}\psi(x)$

Gauge field

Line element

$$ds^2 = dt^2 - a^2(t)\left[\frac{dr^2}{1-kr^2} + r^2d\theta^2 + r^2\sin^2\theta d\phi^2\right]$$

$$\Re^i_k - \frac{1}{2}R\delta^i_k = -\frac{8\pi G}{c^4}T^i_k - \Lambda\delta^i_k$$

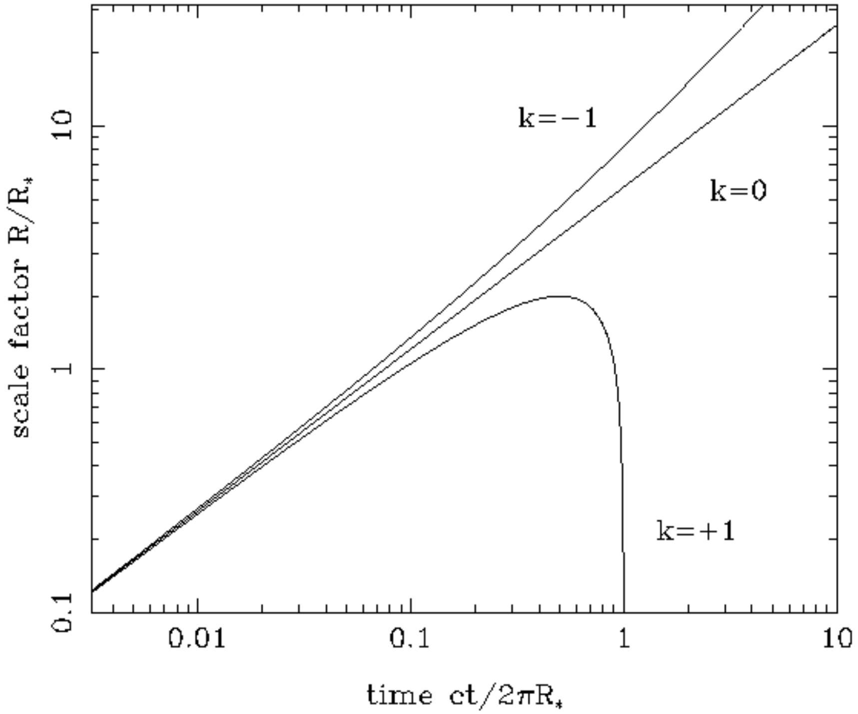

Links STANDARD ⟷ BIG BANG model

	Standard model	LINK	Big Bang models
principle equations	$(i\gamma^\mu\partial_\mu - m)\psi = 0$	–	$\mathcal{R}^i_k - \frac{1}{2}R\delta^i_k = -\frac{8\pi G}{c^4}T^i_k - \Lambda\delta^i_k$
parameter	19	–	11
4 dimensional space	x,y,z,t	yes	x,y,z,t
energy (eV)	E	yes	E
vacuum	V	yes	V
mass	Higgs	–	$T^i_k \neq 0$ for $\Lambda = 0$
momentum	$\bar{p} = -i\hbar\bar{\nabla}$	–	$m\bar{v}$
particle location	$\|\psi\|^2$	–	x,y,z,t
particle size r	$r = 0$	–	$r > l_{Planck}$
particle density ρ	$\rho = \infty$	–	$\rho < \rho_{Planck}$
particle charge	color, EM , weak	yes	color, EM , weak
particle interaction	strong, EM , weak	yes	strong, EM , weak, gravitation
interaction scale Q	$\alpha = f(Q) = f(size)$	yes	$Q = f(size) = f(t_{AfterBigBang})$

Both models are embedded in ONE physic nature and are very successfully.

But until today we have ***NO*** unification.

PARAMETERS of Lambda-CDM model

The 14 parameters of the ΛCDM model decay in two groups. The first 10 parameters are defined by the evolution of the early universe and the second group of 4 parameters are depending about curvature fluctuation, scalar spectral index, redshift fluctuations of galaxies (peculiar velocity) and re-ionization optical depth. (ΛCDM Model Wikipetia 2014)

Evolution of the early universe

Observations suggest the universe at large scales is homogeneous and isotropic with an uniform density ρ (t).

An observer will see, under this isotropy conditions, a point r moving away from him with a speed proportional to the distance from the observer in equ. 1

$$\dot{r}(t) = \mathrm{v}(t) = f(t) \cdot r \qquad (1)$$

Integration of equ. 1 opens the possibility to describe any material body in the universe in the form r (t) = a (t) x, with expansion scale factor $f(t) = \dot{a}/a$, x and r as co-moving coordinates.

The dynamics of the universe is entirely determined by the function a(t). Observations indicate that the relation equ. 2

$$\boxed{v = \left(\frac{\dot{a}}{a}\right) \cdot r = H(t) \cdot r} \qquad (2)$$

does hold in our universe for $\dot{a} > 0$. H(t) is the Hubble constant.

The dynamics of a(t) can be understood from the application of general relativity to a homogeneous and isotropic distribution of matter with ρ as energy density with the metric in equ. 3.

$$ds^2 = dt^2 - a^2(t)\left[\frac{dr^2}{1-kr^2} + r^2 d\theta^2 + r^2 \sin^2\theta d\phi^2\right] \qquad (3)$$

The parameter k modifies the metric of 3-space and the function a(t) scales the distance between any two points in the 3-dimensional space.

The Einstein equations then reduce to the Friedmann equations equ. 4

$$\left(\frac{\dot{a}}{a}\right)^2 = -k\frac{c^2}{a^2} + \frac{8\pi G}{3}\rho(t) + \frac{c^2}{3}\Lambda \qquad (4a)$$

$$2\frac{\ddot{a}}{a} + \left(\frac{\dot{a}}{a}\right)^2 = -k\frac{c^2}{a^2} - \frac{8\pi G}{c^2}p + c^2\Lambda \qquad (4b)$$

The cosmology constant Λ and the pressure p will be ignored in the further discussion.

Expansion of the UNIVERSE after the solution of the Friedmann equations equ.4 for k = -1 , 0 , +1 (Wikipetia 2014)

Expansion of the UNIVERSE as function of the density $\Omega = \rho / \rho_{crit}$ (Wikipedia)

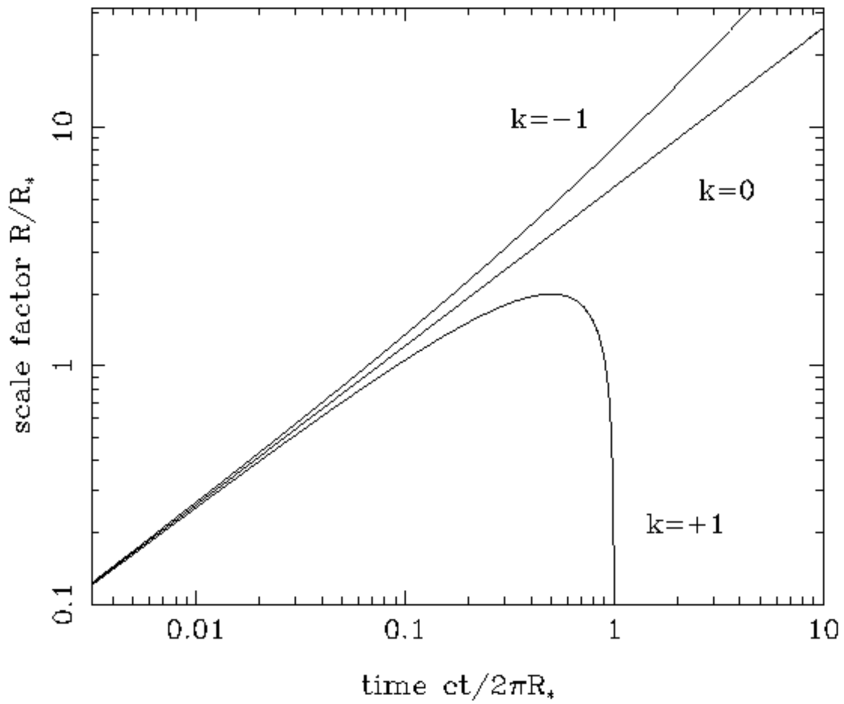

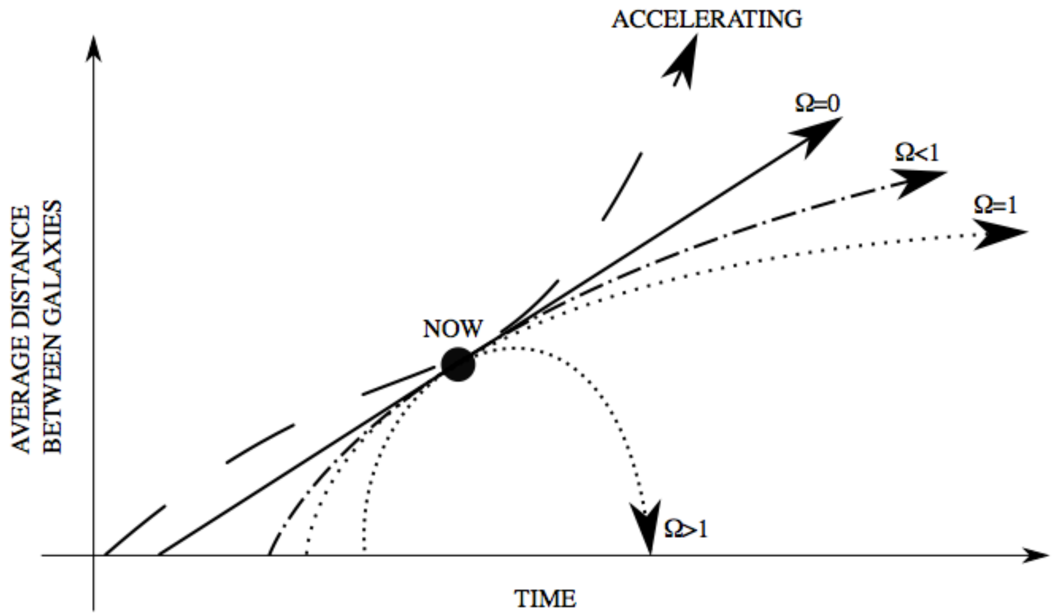

k = -1 the universe expand to ∞
k = 0 the universe stop at ∞
k = +1 the universe BIG CRUNCH

Ω Dark matter accelerating
Ω = 0 No baryon MATTER
Ω < 1 expanding k = -1
Ω = 1 stop at ∞ k = 0
Ω > 1 BIG CRUNCH k = +1

A common value to describe the evolution of the universe is the deceleration parameter $q(t)$shown in equ. 5.

$$\boxed{q(t) = -\left(\frac{\ddot{a}}{a}\right) \Big/ \left(\frac{\dot{a}}{a}\right)^2 = -\frac{1}{H(t)^2}\frac{\ddot{a}}{a}} \qquad (5)$$

To measure all mass and energy densities in the universe it is helpfully to perform this in a ratio to the critical density ρ_c in equ.6

with $$\rho_c = \frac{3H_0^2}{8\pi G} = 1.88h^2 \times 10^{-29}\, gr/cm^3$$

$$\boxed{\Omega_i = \rho_i / \rho_c} \qquad (6)$$

The parameter H_0 is the Hubble constant at the time t_0 today.

The calculation of the development of the densities of the universe it is necessary to find an equation for energy conservation. This is possible via the differentiation of equ. 4a to the time, set this result in equ. 4b and take into the equation of motion $p = \omega\rho c^2$. The parameter ω depends about the type of content of matter. This leads to equ. 7 the equation of energy conservation.

$$\frac{d}{dt}(\rho a^3) = -\frac{p}{c^2}\frac{d}{dt}(a^3) = -\omega\rho\frac{d}{dt}(a^3) \qquad (7)$$

Taken into account all forms of known energy densities at the present universe (Indicated by the subscript ZERO) is than possible to calculate the development of the density Ω_i of the universe as function of the distance parameter a as shown in equ. 8

$$\boxed{\frac{\dot{a}}{a} = H_0^2 \sum_i \Omega_i \left(\frac{a_0}{a}\right)^{3(1+\omega_i)} - \frac{k}{a^2}} \qquad (8)$$

Each matter species is defined by Ω_i and ω_i. For dust is $\omega_i = 0$ and for radiation $\omega_i = 1/3$.

To describe the dynamics of the universe it is necessary to consider four types of densities, the Dark Energy density Ω_V , the Dark Matter density Ω_{DM}, the Baryon density Ω_B and the small contribution of the radiation density Ω_R. These contributions are grouped in a non radiation density ρ_{NR}, a radiation density ρ_R and a vacuum density ρ_V as the sum of the total density ρ_{total} shown in equ. 9.

$$\rho_{\mathrm{total}}(a) = \rho_{\mathrm{R}}(a) + \rho_{\mathrm{NR}}(a) + \rho_{\mathrm{V}}(a) = \rho_c \left[\Omega_{\mathrm{R}} \left(\frac{a_0}{a} \right)^4 + (\Omega_{\mathrm{B}} + \Omega_{\mathrm{DM}}) \left(\frac{a_0}{a} \right)^3 + \Omega_{\mathrm{V}} \right] \quad (9)$$

If equ. 4 and equ. 8 is used, it is possible to write down the development of these densities as function of leading parameter a, a_0,H_0 and k in equ. 10

$$\boxed{\frac{\dot{a}^2}{a^2} + \frac{k}{a^2} = H_0^2 \left[\Omega_{\mathrm{R}} \left(\frac{a_0}{a} \right)^4 + \Omega_{\mathrm{NR}} \left(\frac{a_0}{a} \right)^3 + \Omega_{\mathrm{V}} \right]} \quad (10)$$

To calculate the age of the universe it is possible to find with equ. 4 for k = 0 the relation equ. 11 (Matter universe).

$$\frac{a}{a_0} = \left(\frac{3}{2} \cdot H_0 \cdot t\right)^{2/3} \qquad (11)$$

t is the time , a_0 the value at the time t_0 today. The time is fixed at t_0 today. With equ. 11 is it possible to calculate any time in the past for a given a in particular the age of the universe t_0 for $a_0 = a$ even for small values of $k \neq 0$.

An important parameter to measure the distance to an object in space is the luminosity L or power radiated from an object measured with a POLOMETER in (W), shown in equ. 12 a

$$L = \sigma A T^4 \ (\mathrm{W}) \qquad (12a)$$

with σ as Stefan–Boltzmann constant, A area and T temperature.

It is common to use the luminosity in a special form called the MAGNITUT – luminosity shown in equ. 12 b (Called also brightness from Greek history)

$$m_{star} = m_{\oplus} - 2.5\log_{10}\left[\frac{L_{star}}{L_{\oplus}}\left(\frac{d_{\oplus}}{d_{star}}\right)^2\right] \qquad (12b)$$

with

m_{star} is the apparent magnitude of the star (a pure number)
$m_{\oplus}$ is the apparent magnitude of the Sun (also a pure number)
L_{star} is the visible luminosity of the star
$L_{\oplus}$ is the solar visible luminosity
d_{star} is the distance to the star
$d_{\oplus}$ is the distance to the Sun

The apparent magnitude m_x, in the spectral band x, would be given by:

$$m_x = -2.5\log_{10}\left(\frac{F_x}{F_{x,0}}\right)$$

F_x is the observed flux using spectral filter x, $F_{x,0}$ is 30 Doradus image taken by ESO's VISTA. This nebula has an apparent magnitude of 8. the reference flux (zero-point) for that photometric filter.

Standard apparent magnitudes and fluxes for typical bands[9]

Band	λ (μm)	$\frac{\Delta\lambda}{\lambda}$ (FWHM)	Flux at $m = 0$, $F_{x,0}$ (Jy)	Flux at $m = 0$, $F_{x,0}$ (10^{-20} erg/s/cm^2/Hz)
U	0.36	0.15	1810	1.81
B	0.44	0.22	4260	4.26
V	0.55	0.16	3640	3.64
R	0.64	0.23	3080	3.08
I	0.79	0.19	2550	2.55
J	1.26	0.16	1600	1.6
H	1.60	0.23	1080	1.08
K	2.22	0.23	670	0.67
L	3.50			
g	0.52	0.14	3730	3.73
r	0.67	0.14	4490	4.49
i	0.79	0.16	4760	4.76
z	0.91	0.13	4810	4.81

https://en.wikipedia.org/wiki/Apparent_magnitude

Example of Apparent magnitude

30 Doradus image also called Tarantula Nebula taken by ESO's VISTA.

The nebula has a apparent magnitude of 8

https://en.wikipedia.org/wiki/Apparent_magnitude. ESO/M.-R. Cioni/VISTA Magellanic Cloud survey – http://www.eso.org/public/images/eso1033a/

An important parameter is the distance to an object in space r measured via the magnitude luminosity m_x of the object equ. 12c

$$m - M = 5 \cdot \log \frac{r[pc]}{10} = 5 \cdot \log r[pc] - 5 \qquad (12c)$$

M is the magnitude of a known standard candle (Star, Galaxy a.s.o.).
r is inserted in units of 10 Parsec [pc]. ($1 pc = 3.086 \times 10^{16} m$)

If the universe expand the stars and galaxies will move away from each other. The leading parameter to describe this fact is the RED-SHIFT z_e. A source moving away from an observer will emit a radiation with a frequency ν_e and a wave length λ_e. An observer today will receive a radiation with a frequency ν_0 and a wave length λ_0. This fact is connected to the important parameter a by the equ. 13.

$$1 + z_e = \frac{\lambda_0}{\lambda_e} = \frac{\nu_e}{\nu_0} = \frac{a_0}{a(t)} \qquad (13)$$

For a source of the light moving away from an observer redshift $z > 0$,if the moves towards blueshift $z < 0$ occurs. For a source what moves away from the observer with velocity v, which is much less than the speed of light ($v \ll c$), the redshift is given by the Doppler Red shift.

$$z \approx v/c \qquad \gamma \approx 1 \qquad (13a)$$

For the relativistic Doppler effect the equation is

$$1 + z = \left(1 + \frac{v}{c}\right) \cdot \gamma \qquad \gamma = \frac{1}{\sqrt{1 - \frac{v^2}{c^2}}} \qquad (13b)$$

Substantial effort in experiment was spent to measure the Hubble constant H (t).
This is possible with equ. 12c, 13a and 13b.

$$v = H(t) \cdot r$$

The measured Red Shift z of an object allows via equ. 13a to define the velocity v.

$$z \approx v/c \qquad \gamma \approx 1$$

and the distance r to the object can be measured via the magnitude luminosity m_x equ. 12c

$$m - M = 5 \cdot \log \frac{r[pc]}{10} = 5 \cdot \log r[pc] - 5$$

With the known velocity v *and the disdance* r of an object it is possible to calculate H (t).

To describe in a first simple approximation the evolution of the cosmos it is necessary to connect the time t, z and the temperature of the universe T to the leading parameter a, this shown in equ. 14.

$$\frac{a(t)}{a_0} = \left(\frac{t}{t_0}\right)^{1/2} = \frac{1}{1+z(t)} = \frac{T_0}{T(t)} \qquad (14)$$

Evolution of the COSMOS

Including the inflation and primordial nucleon syntheses it is possible to distinguish eight time intervals of the development of the universe :

Inflation : Provides a natural mechanism for the generation of scalar density fluctuations that seed large scale structures.
(Temperature anisotropies in the CMB and primordial gravitational waves)

Primordial nucleon synthesis :

Provides the creation of nucleons and elements as function of the temperature of the universe.

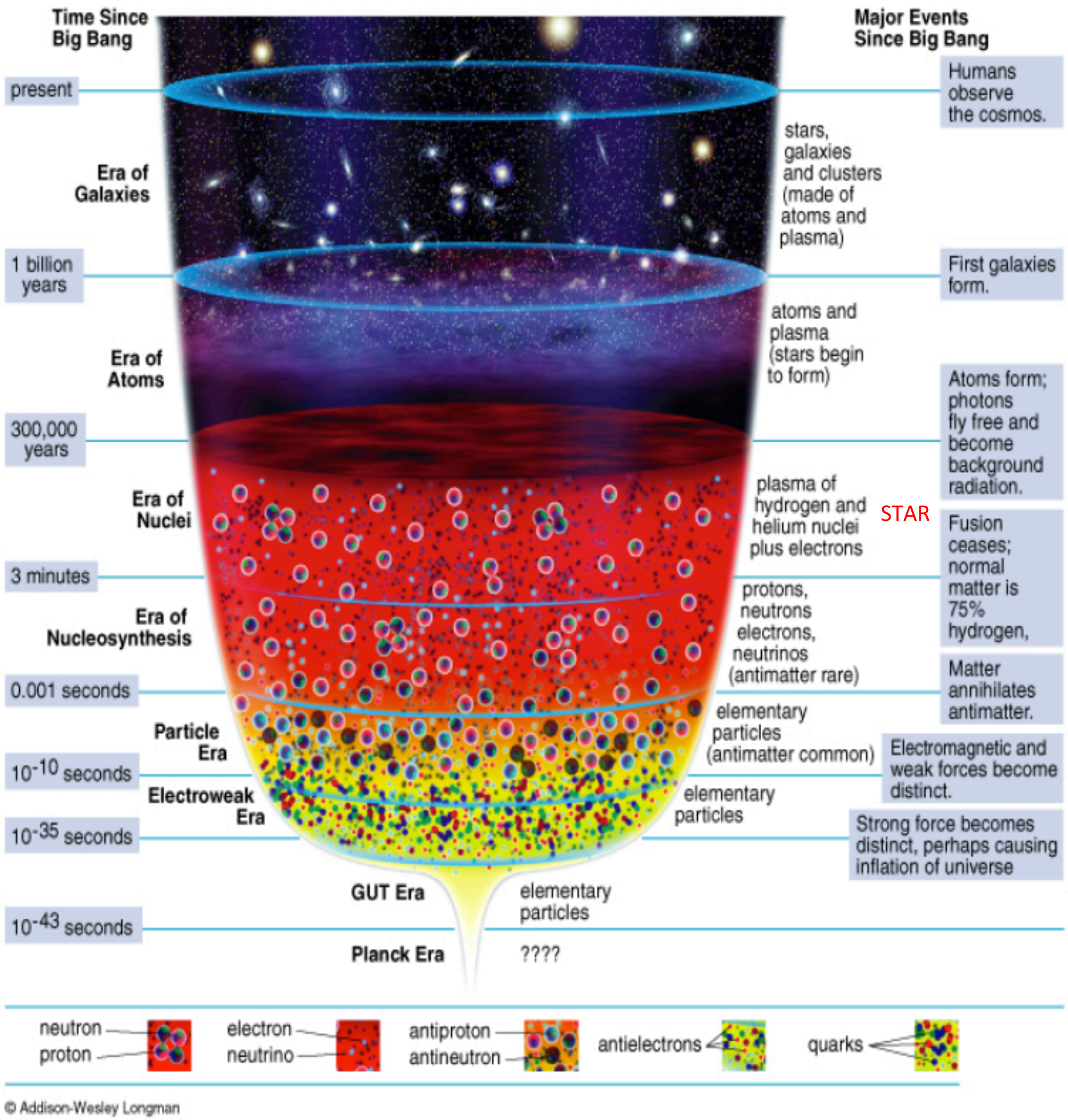

Using the equ. 1 to equ. 13 and the picture below it is possible to visualize the first 10 parameters on the ΛCDM model. (ΛCDM Model Wikipetia 2014)

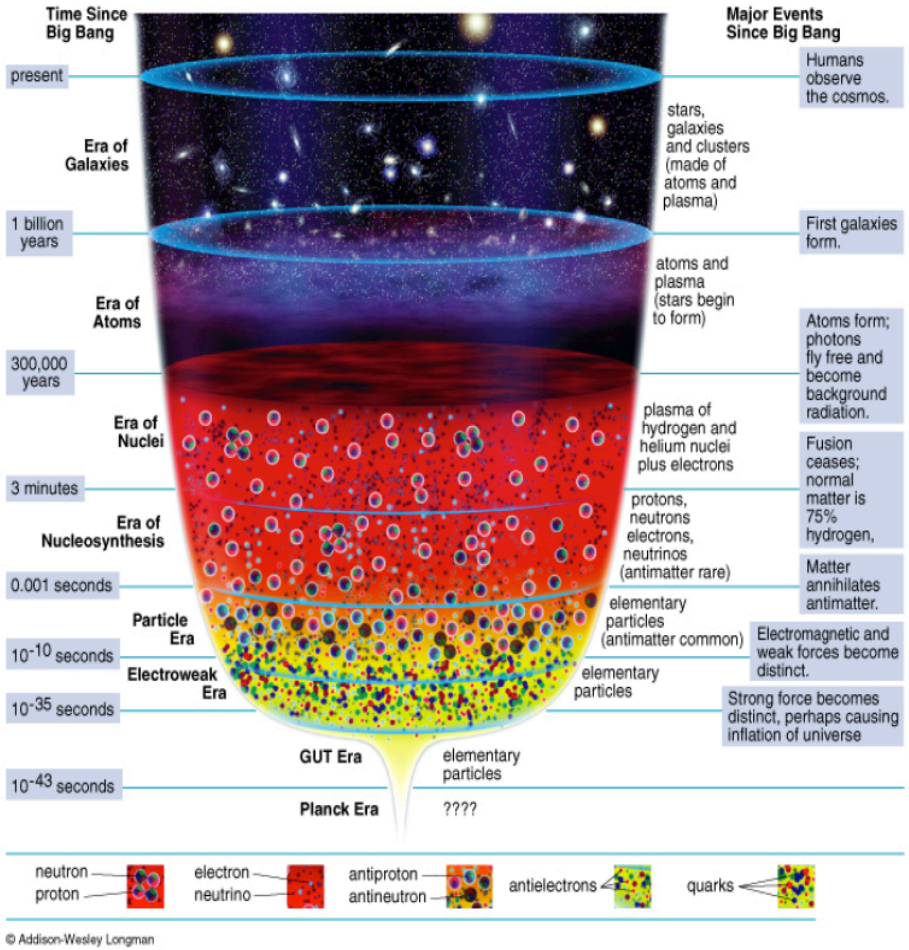

- t_0 Age of the universe.
- H_0 Hubble constant
  (H_0 = h x 100 km/(s Mpc)
- $\Omega_b h^2$ Physical baryon density.
- $\Omega_c h^2$ Physical dark matter density.
- Ω_b Baryon density.
- Ω_c Dark matter density.
- Ω_Λ Dark energy density
- z^* Redshift at decoupling. If the universe is cold enough to form hydrogen.
- t^* Age at decoupling.
- z_{reion} Redshift of re-ionization, measured for example highest redshift quasars.

The final 4 parameters need a different consideration of the discussion so far.

Strategy to search for Dark Matter

As discussed observations suggest the universe at large scales is homogeneous and isotropic with an uniform density ρ (t).

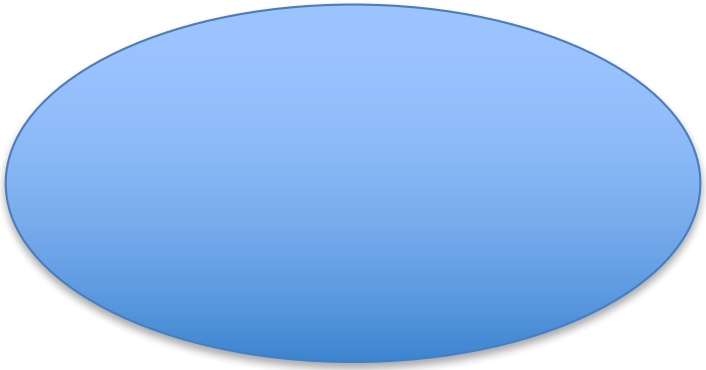

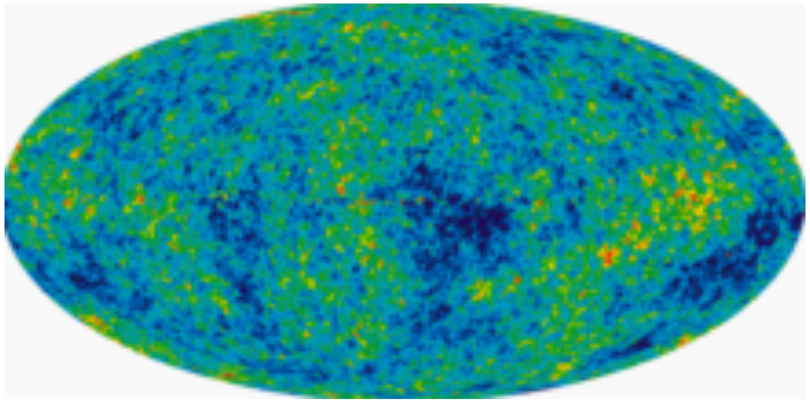

Volume Explosion. The temperature today T ≈ 2.73 K

Very tiny distortion on the homogeneous isotropic universe responsible for galaxies and stars. Δ T ≈ 0.0002 K

The tiny fluctuation originate waves in the density of the universe also in the Dark Matter. A multipol analysis of these waves allows to study the parameters of the ΛCDM model. The parameter of the ΛCDM are strongly depending from the Dark Matter.

The curvature fluctuation parameter Δ_R^2 and the spectral index n_s

The primordial spectral index is linked to gravitational waves. For a power-law spectrum of primordial curvature perturbations $\Re_k$ the parameter is shown in equ. 15.

$$\Delta_{\Re}^2(k) = \frac{k^3 \left\langle \left|\Re_k\right|^2 \right\rangle}{2\pi^2} = \Delta_{\Re}^2(k_0)\left(\frac{k}{k_0}\right)^{n_s-1} \qquad (15)$$

with k as wavenumber and n_s the scalar spectral index. ($\Delta_{\Re}^2(k)$ and n_s first two parameter) (arXiv:1001.4538v3 [astro-ph.CO] 9 Nov 2010)

The fluctuation between peculiar velocity and density fields of galaxies σ_8

The relationship between the peculiar velocity v_p of galaxies velocity field and the density field for a linear regime is shown in equ. 16 (Peebles 1980 Princ. of Physic. Cos. Princeton Uni. Press)

$$v_p(r) = \frac{\beta}{4\pi}\int d^3r' \frac{\delta_g(r')(r'-r)}{\left|r'-r\right|^3} \qquad (16)$$

The galaxy number density fluctuation field δ_g is related mass density fluctuations field by $\delta_g = b\delta$ and $\beta = \Omega^{0.6}/b$ with b as biasing parameter. The parameter β is relate to the maximum fluctuation amplitude σ_8. (σ_8 third parameter)

Reionization optical depth

Observations of the spectra of distant quasars and galaxies show that the intergalactic medium was highly ionized at redshifts of about $z = 5$. Since the universe get neutral at $z \approx 1000$ the intergalactic medium should stay neutral until it is reionized through active luminous source. If for example hydrogen get ionized the Thomson scattering of light on the electrons will change the transparency of the universe, in particular the " Surface brightness " of an object.

Candidates for such a source could be quasars, supernova-driven wind, cosmic rays and stellar reionization.

A short summery of a stellar reionization model (A. Venkatesan, The Astrophys. J., 537 (2000) 55) is discussed next.

A fraction F_B of baryons, in a collapsed dark matter halo, form stars. A fraction of the generated ionizing photons escape isotropically into the intergalactic medium. It then possible to define a filling factor of ionized hydrogen by the volume $F_{H\,II}$. For a homogeneous intergalactic medium the ionized region can be approximated by a sphere of radius r_i. The reionization is defied to occur when $F_{H\,II} = 1$. The total optical depth for electron scattering τ_{reion}, to the reionization redshift z_{reion} is than the integral over the electron density, the ionization fraction, the Thomson cross section from z today to z_{reion} shown in equ. 17

Thomson scattering (Elastic scattering)

$$\gamma + e \rightarrow \gamma + e \qquad \sigma_t \equiv \frac{8\pi}{3} r_e^2$$

Ionization

$$\gamma + H \rightarrow p + e + \gamma$$

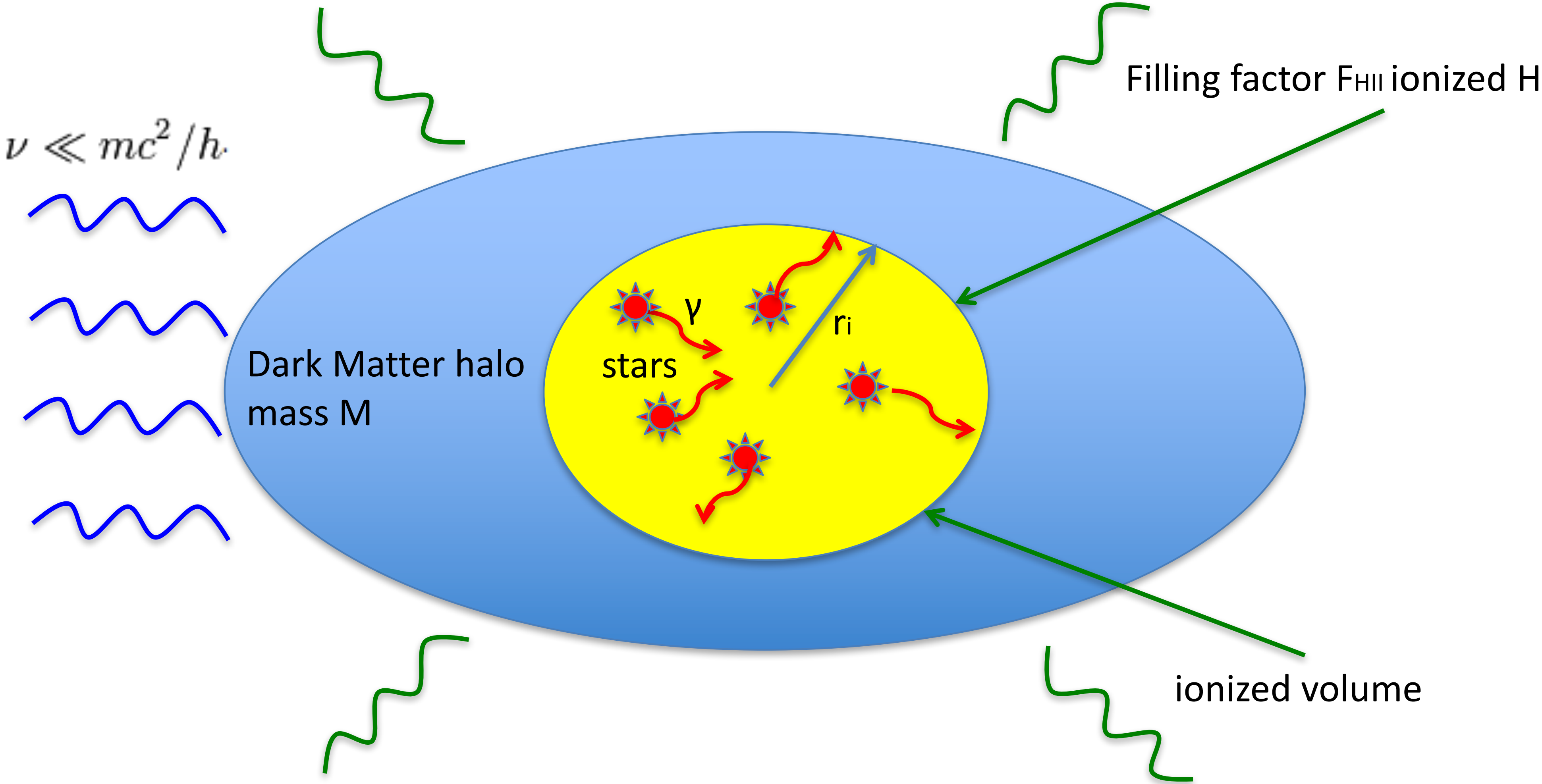

$$\tau_{rion} \approx \rho_e \cdot F_{HII}(z) \cdot \sigma(Thomson) \qquad (17)$$

The fourth parameter is the Reionization Optical Depth τ_{reion}

$$F_B(z) = erfc\left[\frac{\delta_c}{\sqrt{2}\cdot\sigma(R,z)}\right] \quad \rightarrow \quad erfc(x) = \frac{2}{\sqrt{\pi}}\int_x^{\infty} e^{-t^2}\,dt$$

$$F_{HII} = \rho_B(z)\int_{z^*}^{z} dz_{on}\,\frac{dF_B}{dz}(z_{on})\left[\frac{4\pi}{3M}r_i^3(z_{on},z)\right] \qquad (17\ a)$$

$$\tau_{reion} = 0.053\cdot\Omega_b\cdot h\int_0^{z_{reion}} dz\sqrt{1+z}\cdot\left[1-f^*F_B(z)\right]F_{HII}(z)$$

- $F_B(z)$ Fraction of baryons in collapsed dark matter halo.
- δ_c Critical over density.
- $\sigma(R,z)$ Thomson cross section.
- $F_{HII}(z)$ Filling factor of ionized hydrogen volume.
- $\rho_B(z)$ Baryon density.
- z^* Earliest redshift stars can form.
- M_c Minimum halo mass that collapses at a given redshift.
- r_i Radius of ionized region.
- $0.053\Omega_b$ Electron density. (Reduced Ω_b Baryon density)
- h Reduced Hubble constant.
- z_{reion} Redshift where the reionization occur.
- f^* Fraction of baryons which cool and form stars.

These are all 14 parameters of the Lambda-CDM model. In a global fit the model optimizes all these parameters in comparison with the observations. Even if the observations restrict the parameter space, a 14 dimensional fit needs big effort to find optimal solutions and it is not surprising if multiple solution are possible. Under this circumstances are many discussion on the way to improve this model.

As example a Lagrangian for the Lambda CDM Model introduced be H. F. Farmer (viXra:1106.0041) is shown in equ. 18 including the Einstein equation.

Ricci curvature Scalar Field EM Field Vector Field

$$s = \int \sqrt{-g}\left(-\frac{R}{16\pi} - k(\phi)\nabla^{\mu}\phi\nabla_{\mu}\phi - \frac{1}{4}F^{\mu\nu}F_{\mu\nu} - \frac{1}{2}\left(m_{\phi}^{2}\phi^{2} + m_{A}^{2}A^{\mu}A_{\mu}\right) - \frac{R}{6}\left(\phi^{2} + A^{\mu}A_{\mu}\right)\right) d^{4}x$$

$$\boxed{A^{\mu} = A^{\mu}(R), \phi = \phi(R)}$$

$$m_A = \sqrt{\frac{-R}{3}}$$

$$m_{\phi} = \sqrt{\frac{6\lambda\Lambda - R\phi}{3\phi}}$$

$$R^{\mu\nu} - Rg^{\mu\nu} = \frac{8\pi G}{c^2}T^{\mu\nu}$$ ENERGY

$$\nabla_{\alpha}F^{\alpha\mu} - \left(\frac{m_A^2}{2} + \frac{R}{6}\right)A^{\mu} = 0$$ Vector Field

$$\nabla_{\mu}\nabla^{\mu}\phi - \left(\frac{m_{\phi}^2}{2} + \frac{R}{6}\right)\phi = 0$$ Scalar Field

$$T^{\mu\nu} = \lambda g^{\mu\nu}\Lambda$$

(18)

$$T^{\mu\nu} = -2k(\phi)\nabla^{\mu}\phi\nabla^{\nu}\phi - F^{\mu\nu}g_{\lambda\delta}F^{\lambda\delta} - \left(m_A^2 + \tfrac{R}{3}\right)A^{\mu}A^{\nu}$$
$$-g^{\mu\nu}\left(k(\phi)\nabla_{\mu}\phi\nabla^{\mu}\phi + F^{\mu\nu}F_{\mu\nu} - \tfrac{1}{2}\left(m_{\phi}^{2}\phi^{2} + m_{A}A^{\mu}A_{\nu}\right) - \tfrac{R}{6}\left(\phi^{2} + A^{\mu}A_{\mu}\right)\right)$$

The parameters of the ΛCDM model get restricted by 8 observations

- The galactic rotation curves.
- Velocity dispersion of galaxies and galaxy redshift survey σ_8
- Galaxy clusters and gravitational lensing.
- Cosmic microwave background, ΔR and n_s.
- Sky surveys and baryon acoustic oscillations.
- Type Ia supernovae distance measurements, H_0 and τ.
- Lyman-alpha forest.
- Structure formations.

The galactic rotation curves

It is known since Fritz Zwicky (1933) that the rotational curves of galaxies can only be explained be introducing a mass halo close to centre of the galaxy. Two examples of the galaxy NGC 6503 and NGC 3196 are shown in fig. 1.

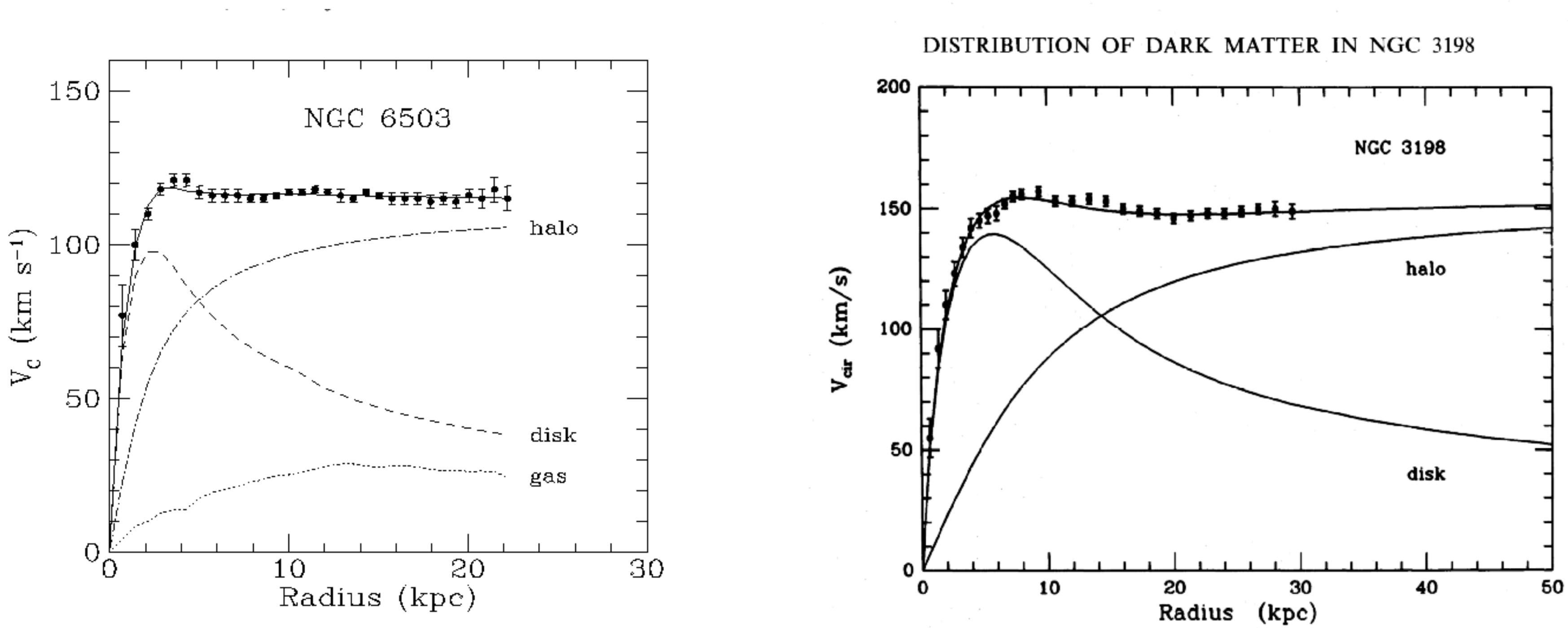

Fig. 1 Galactic rotational curve from NGC 6503 (antares.in2p3.fr) and NGC 3196 (bustard.phys.nd.edu).

Low Surface Brightness LSB galaxies are probably everywhere dark matter dominated

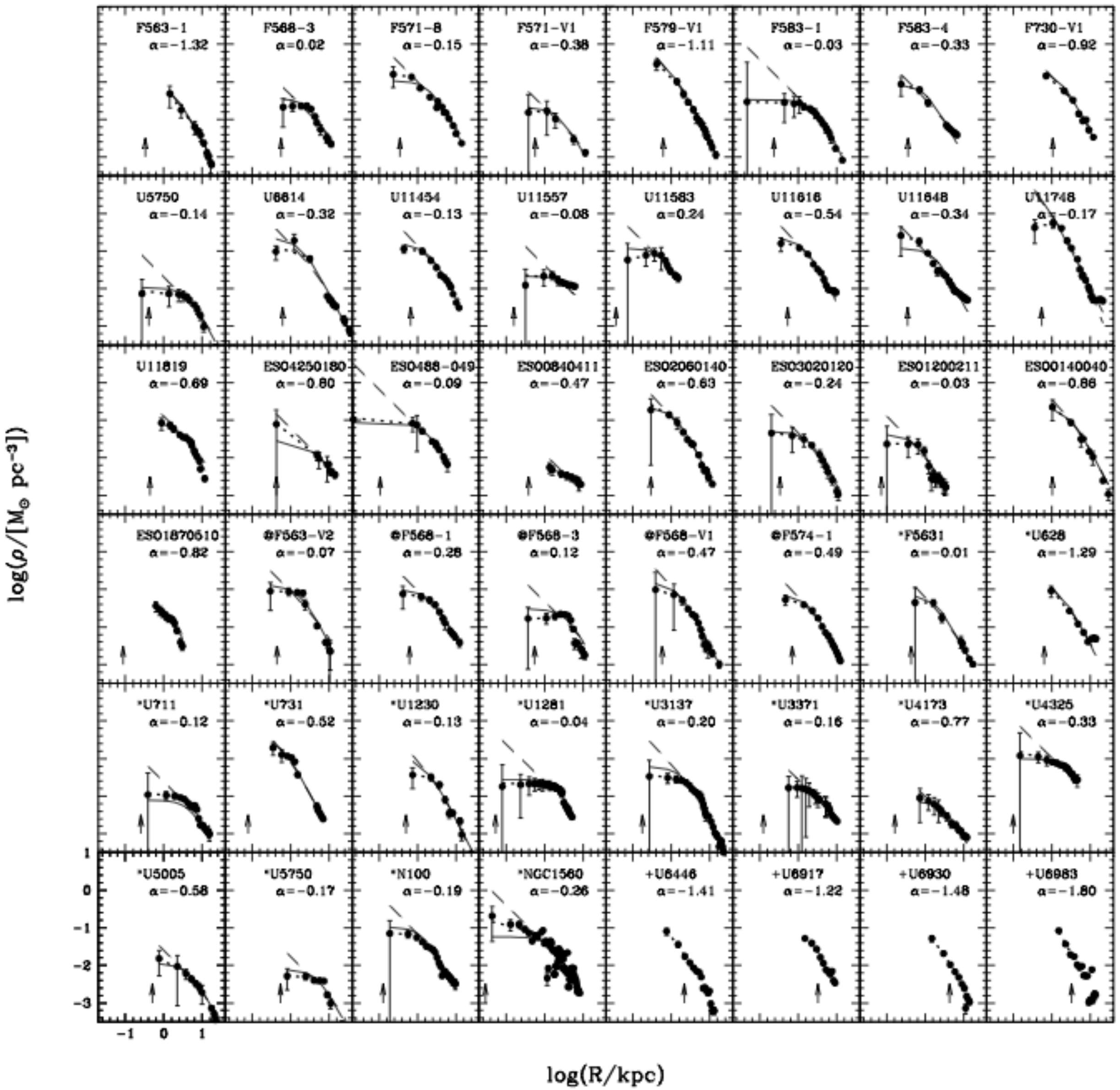

Fig. 2 Mass profiles of LSB galaxies (Points) and rotation curves (Solid line).
(arXiv:astro-ph/0103102v2 9 Mar 2001)

The investigation of the LSB allows to estimate the mass density distribution

$$\boxed{\rho(r) \approx r^{\alpha}}$$

Spiral Galaxies (Fig. 3) rotational curves suggest a universal density profile. The profile could be described by an overlay of a stellar disk and a spherical dark halo with a flat core of radius r_0.

$$\boxed{\rho_0 = 4.5 \times 10^{-2} (r_0/\mathrm{kpc})^{-2/3}\ M_{\odot}\mathrm{pc}^{-3}}$$

With M⊙ as solar mass

This density profile is linked to the parameters Ω_m, Ω_Λ and h of the ΛCDM model.
(arXiv:astro-ph/0203457v1 26 Mar 2002)

Fig. 3 Spiral galaxy NGC 5457 (STScl-PRC2006-10a.jpg)

Elliptical galaxies show evidence for dark matter via strong gravitational lensing (gravitational lensing will be discussed later). X-ray evidence reveals the presence of extended atmospheres of hot gas that fill the dark haloes what supports evidence for dark matter. But some have low velocities in their outskirts and are interpreted as not having dark matter haloes. More investigation is necessary. As example the galaxy 325-G004 is shown in fig. 4.

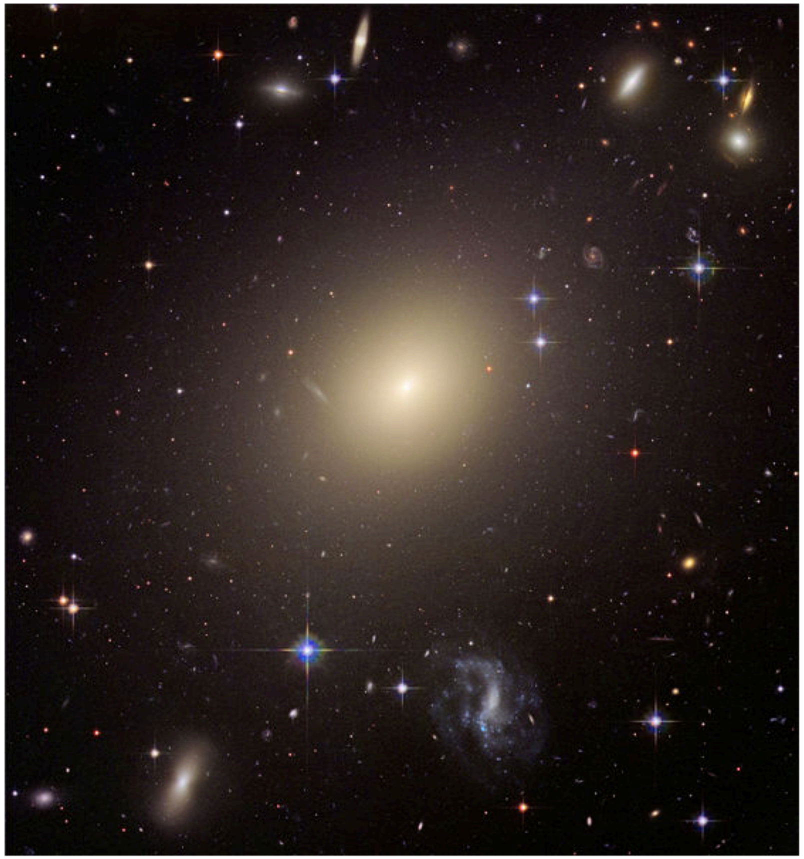

100 eV < X-ray < 100 keV

Fig. 4 Elliptical galaxy ESO 325-G004.jpg

Velocity dispersion of galaxies and Galaxy Redshift Survey σ_8

The velocity dispersion σ is the statistical dispersion of velocities about the mean velocity of objects like open clusters, globular clusters, galaxy, galaxy clusters or super-clusters. By measuring the radial velocities of the objects, the velocity dispersion can be used to derive the mass of the cluster (Virialization, The Astrophys. J.,532 (2000)728). The radial velocity is measured be Doppler with of spectral lines of a collection of objects. The size of σ ranges from the Milky way black hole σ = 75 km/s to elliptical galaxies $\sigma \approx$ 200 km/s.

Measurement of elliptical galaxies (The Astrophys. J., 204 668) indicate a relatively high dark matter content. But there are some galaxies whose velocity profile indicate an absence of dark matter. There is evidence that there are 10 to 100 times less small galaxies than permitted by dark matter theory of galaxy formation predicts (arXiv:astro-ph/9907411). This is discussed under the dwarf galaxy problem.

The fluctuation between peculiar velocity and density fields of galaxies σ_8 we discussed in equ.16. The fluctuations $v_p(r) = f (\beta \approx \sigma_8 , \delta g)$. An all-sky redshift survey of 5313 galaxies from the Infrared Astronomical Satellite (IRAS) give an overview of about the β value as function of the inflowing objects to outflowing objects. An example of the analysis of the IRAS data is shown in fig. 5 (arXiv:astro-ph/9801307v1, new data from 2013 in arXiv:1307.1659v2 [astro-ph.CO] 19 Jul 2013)

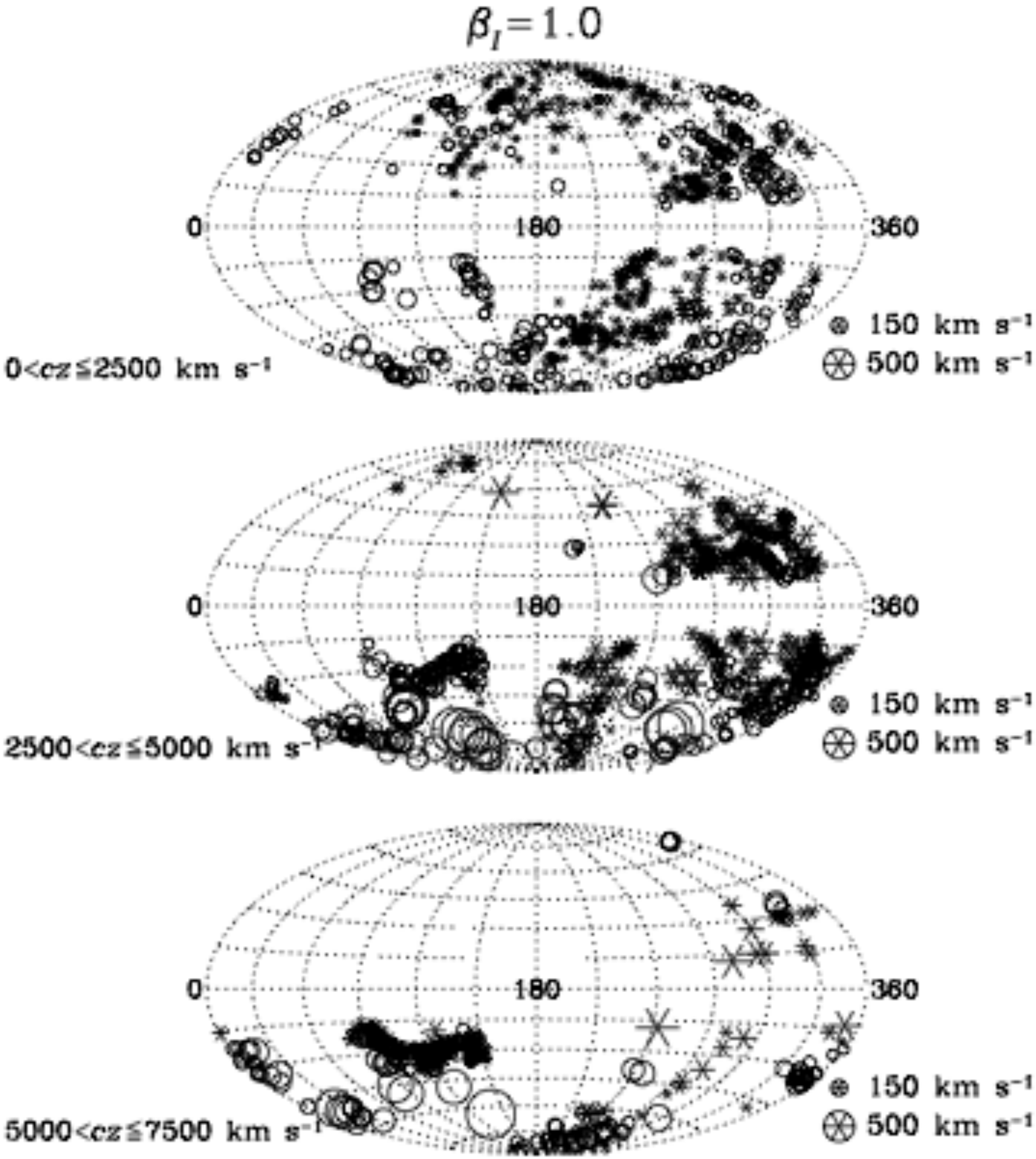

$$v_p(r) = \frac{\beta}{4\pi}\int d^3r' \frac{\delta_g(r')(r'-r)}{|r'-r|^3}$$

$\beta_I \approx \sigma_8$

Fig. 5 Smoothed VELMOD velocity in Galactic coordinates, for β_I = 1.0. Open circles are inflowing objects, starred outflowing objects. The symbol size indicates the magnitude of the velocity.

Galaxy clusters and gravitational lensing

Dark matter affects also galaxy clusters and X-ray spectra of these clusters. An example is shown in fig. 6 from the Abell 2029 cluster (Abell 2029: Hot News for Cold Dark Matter).

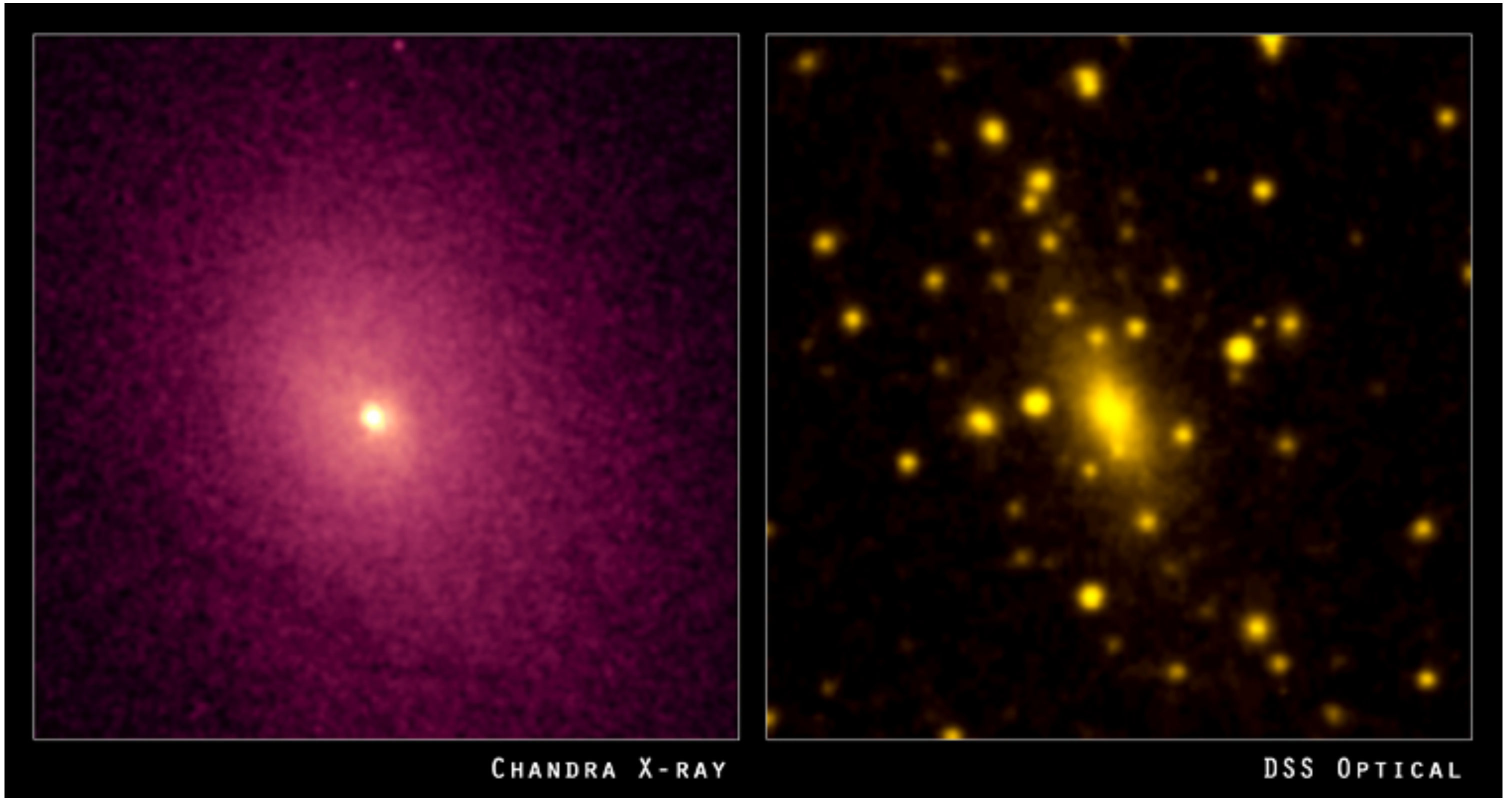

Fig. 6 The Abell 2029 galaxy cluster X-ray (100 eV < X-ray < 100 keV) left optical image right.

The Abell 2029 cluster is composed of thousands of galaxies enveloped in a cloud of hot gas. The amount of dark matter is more as 10^{14} suns.

An further important tool for dark matter observations is gravitational lensing shown in fig. 7 .

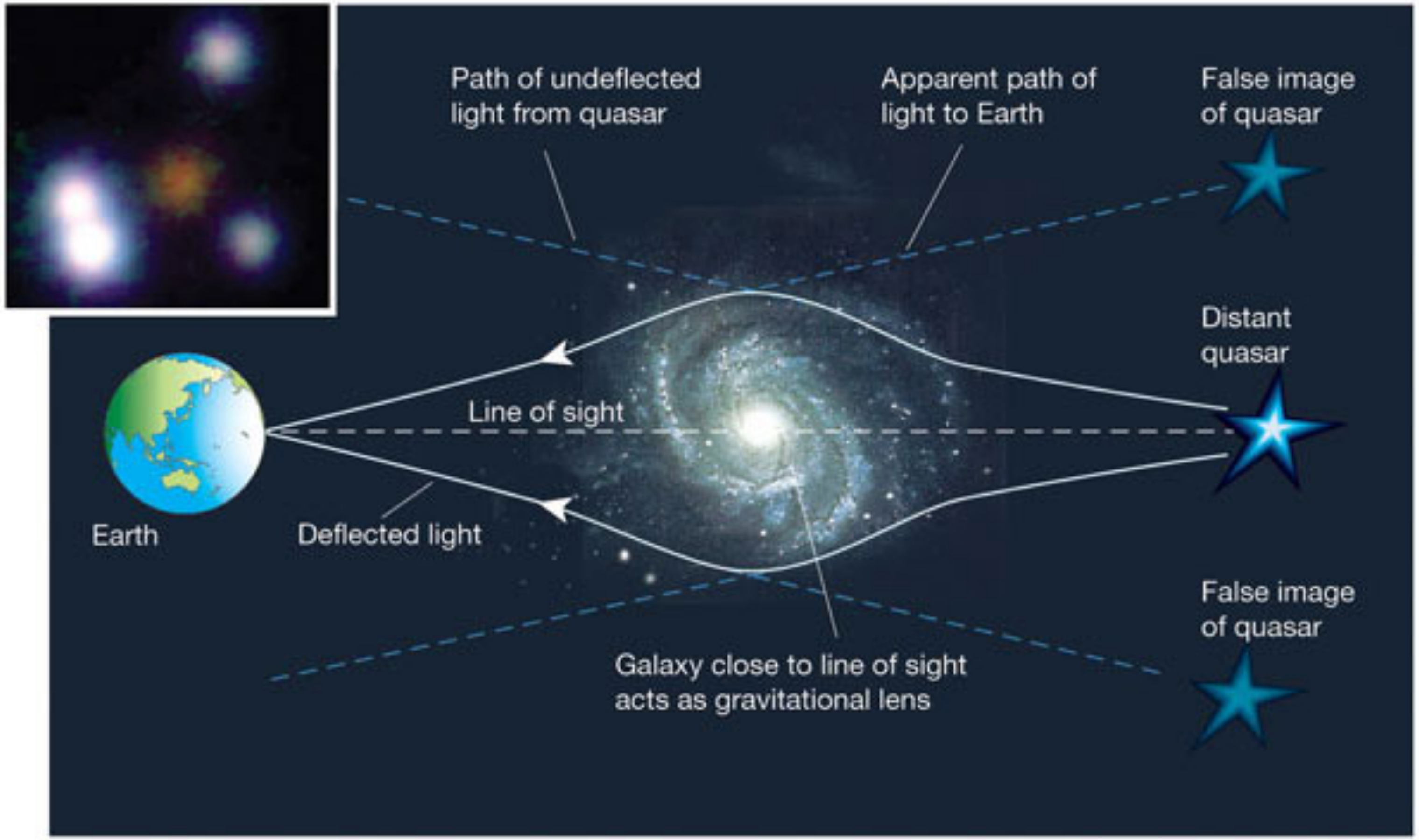

Fig. 7 Schematic view of gravitational lensing.

By examining the apparent shear deformation of the adjacent background galaxies it is possible characterize the mean distribution of dark matter.

The Bullet Cluster in fig. 8 is the most direct observational evidence today for dark matter.

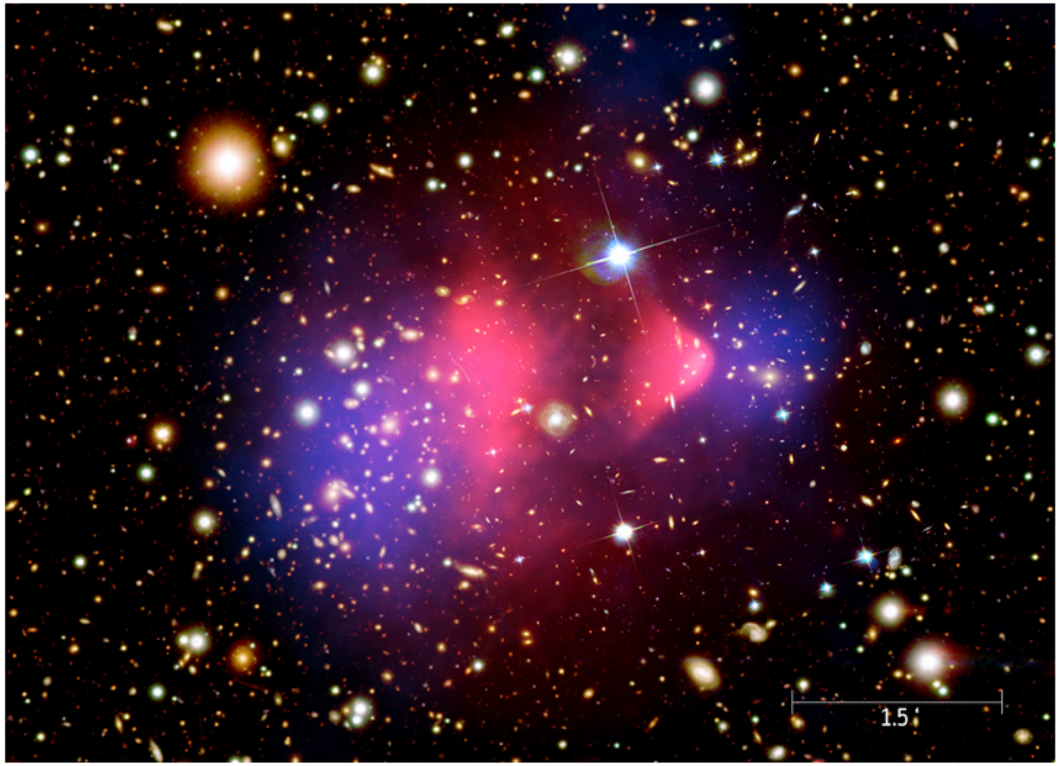

Fig. 8 The Bullet Cluster (Wikipedia **1E 0657-558)**The total mass distribution shown blue, X-ray red.

The Bullet Cluster is a collision between two galaxy clusters appears to have caused a separation of dark matter and baryonic matter. The electromagnetic interaction between passing gas particles caused them to settle near the point of impact in the centre. Dark matter does not interact by electromagnetic forces as visible in the X-ray, the dark matter components of the two clusters passed through each other without slowing down substantially. (See also arXiv:astro-ph/0608407v1 19 Aug 2006)

Cosmic microwave background.

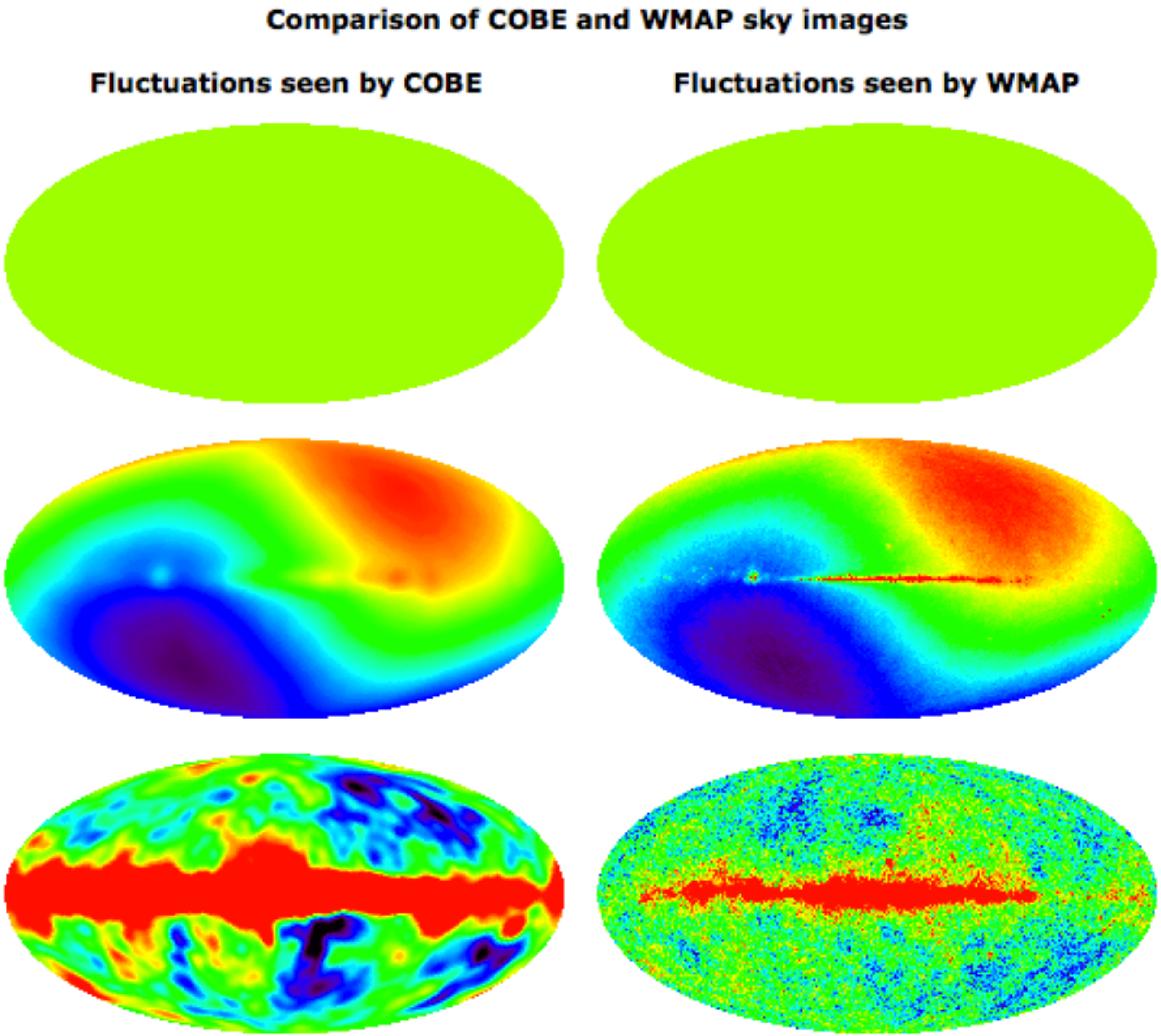

http://map.gsfc.nasa.gov/universe/bb_cosmo_fluct.html

Cosmic microwave background, ΔR and n_s.

The WMAP (E. Komatsu et. al. arXiv:astro-ph/0803.0547) measurement in fig. 9 are the key to establish the current Standard Model of Cosmology Λ-CDM. A flat universe dominated by dark energy, dark matter and atoms with density fluctuations seeded by a Gaussian adiabatic nearly scale invariant process. The detector measured the temperature of the microwave background of 2.7 K with a precision of 5×10^{-5}.

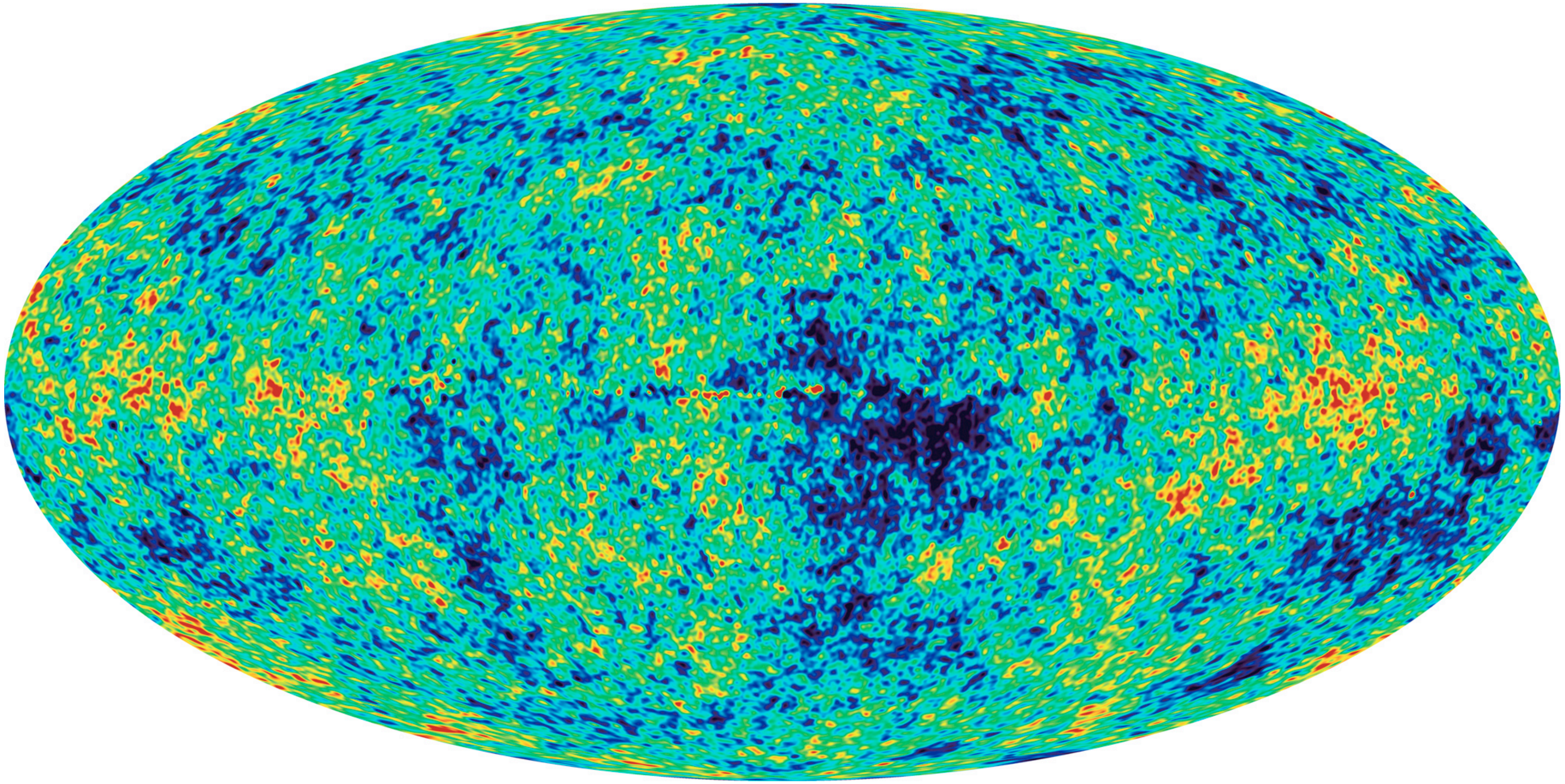

Fig. 9 The WMAP microwave background.

ANGULAR POWER SPECTRUM CALCULATION

CBR Anisotropy is discussed 1995 in a publication from astro-ph/9504071 as a temperature fluctuation.

$$\delta T(\Omega)/T = \sum_{lm} a_{lm} Y_{lm}(\Omega)$$

The variance $C_l \equiv \langle |a_{lm}|^2 \rangle$ serves to specify all statistical properties of the fluctuation.

In the 9 years date analysis, the Fermi LAT group uses an angular power spectrum C_l of an intensity map $I(\psi)$ where ψ denotes the sky direction. The angular power spectrum is given by the coefficients $C_l = \langle |a_{lm}|^2 \rangle$, with the a_{lm} determined by expanding the map in spherical harmonics.

$$\boxed{I(\psi) = \sum_{lm} a_{lm} Y_{lm}(\psi)}$$

The intensity angular power spectrum is compared with predictions for source classes discussed in previous section of the ΛCDM model.

Fermi LAT:arXiv:1202.2856v1 [astro-ph.HE] 13 Feb 2012

The anisotropies in the CBR are explained as acoustic oscillations in the photon-baryon plasma. These oscillations get visible until today after the universe get transparent for light. Baryonic matter interacts strongly with radiation whereas dark matter interacts with gravity. Both interactions have a very different strength. This separates the different contributions of dark energy, dark matter and baryonic matter. In fig. 10 the power spectrum of the CBR anisotropies show a large first peak and smaller successive peaks. The first peak is depending of the density of baryonic matter and the third peak mostly about the density of dark matter.

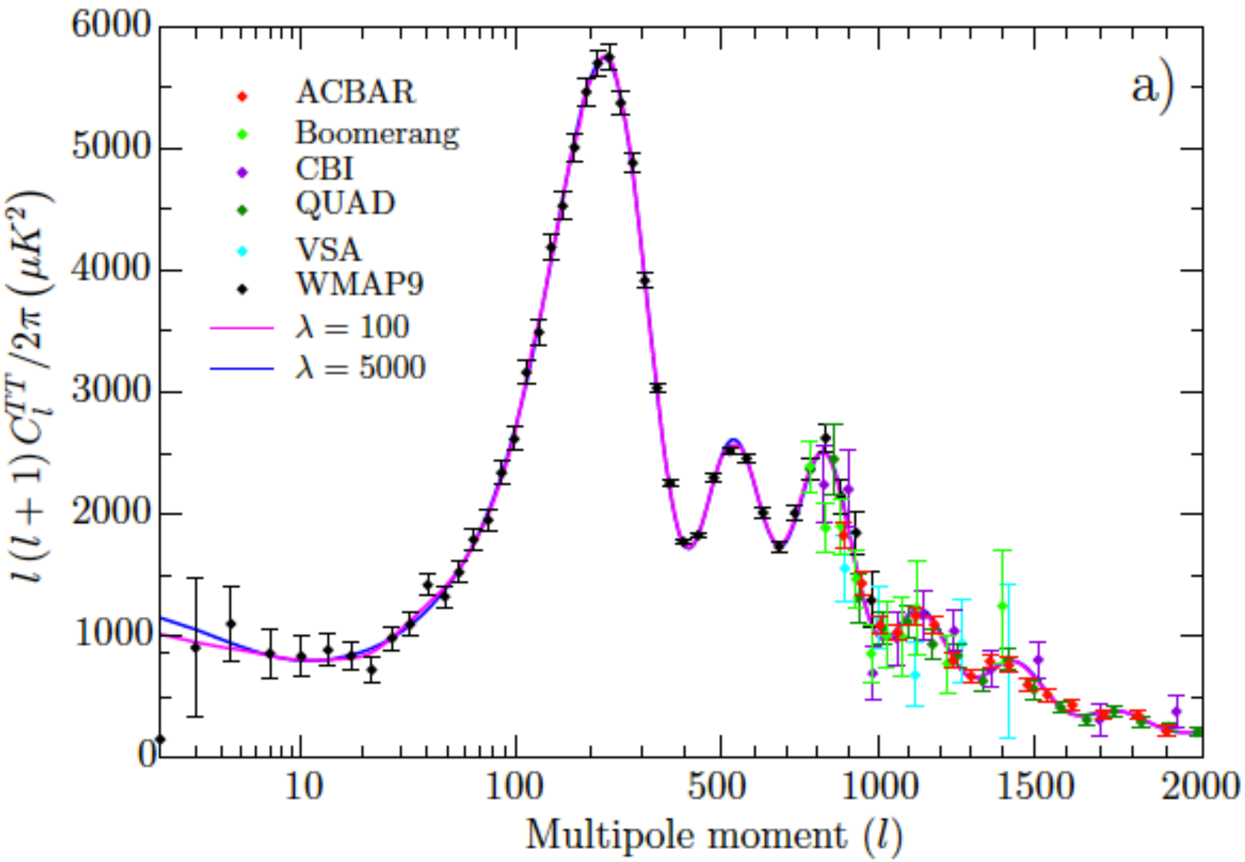

Fig. 10 The multipole power spectrum of six detectors from ref. JCAP01(2014)025.
(λ regularisation parameter)

Inflationary models predict scale-invariant spectra of density perturbations and gravity wave perturbations. Both perturbations contribute to the CBR anisotropy. The leading parameter are the curvature perturbation $\Delta\Re_k$. In the discussion of the fluctuations of gravitational waves of equ. 15 it was demonstrated that also this fluctuation can be developed in a power spectrum very similar to the just discussed power spectrum. As an example is shown in fig. 11 calculation of a power spectrum for an chaotic inflation (arXiv:astro-ph/9504071v2) .

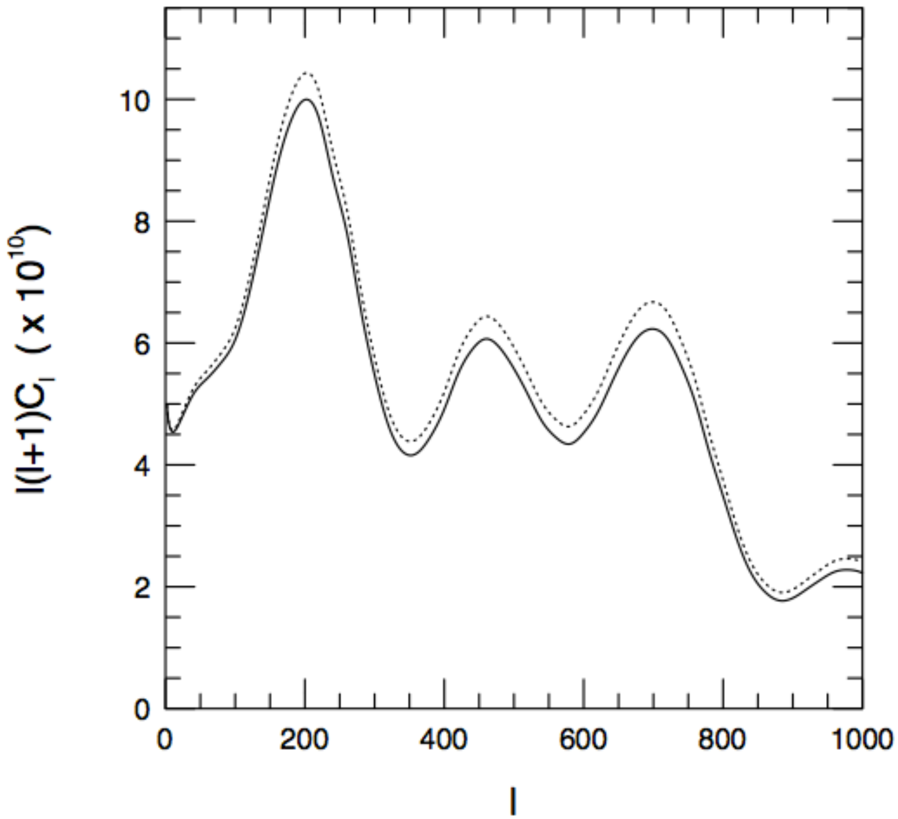

$$\Delta^2_{\Re}(k) = \frac{k^3\left\langle\left|\Re_k\right|^2\right\rangle}{2\pi^2} = \Delta^2_{\Re}(k_0)\left(\frac{k}{k_0}\right)^{n_s-1}$$

Fig. 11 Calculated angular power spectra for chaotic inflation (solid line) and with running scalar spectral index n = 0.92, h = 0.7, Ω_B = 0.025 and dn/d lnk = - 0.002 (broken line)

Sky surveys and baryon acoustic oscillations

The acoustic oscillations occur in the primordial cosmological perturbation, where excite sound waves in the relativistic plasma of the early universe. This leave their imprint in the visible matter by Baryon Acoustic Oscillation BAO clustering. The are measured with sky surveys like the Sloan Digital Sky Survey and the 2dF Galaxy Redshift Survey. These measurement are consistent with the CBR WMAP measurements but confirm the WMAP measurements on a very different distance scale. As example of the result of such an analysis is shown in fig. 12. (arXiv:0907.1660v3)

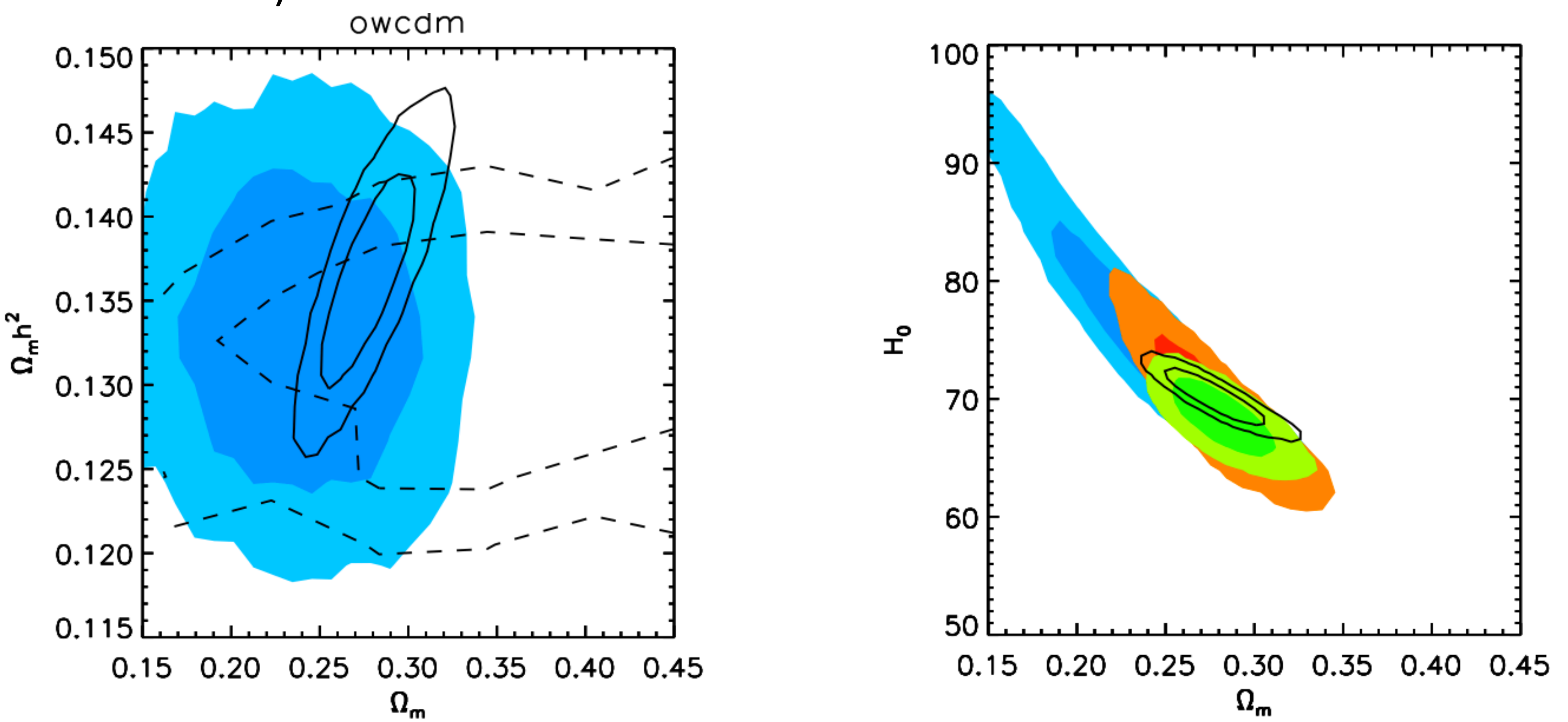

Fig. 12 WMAP+BAO constrains on $\Omega_m h^2$, Ωm and H0. ΛCDM solid black contours, oΛCDM green, wCDM red, owCDM blue and WMAP5 only constrained dashed. (Ω_m=Ω_c+Ω_b)

Type Ia supernovae distance measurements, H_0 and τ

Type Ia supernovae are used as STANDARD CANDLE to measure extragalactic distances. This is important for a independent measurement of H_0, measure the reionization optical depth τ_{reion} , Ω_Λ (Next Seminar) and an extensive data sets of this supernovae are used to constrain CDM-models.

The Virgio Cluster offers the two parameters are v and D to measure the Hubble constant via $v = H_0 \cdot D$ in equ. 2 , 12c and 13. The velocity v is measured via the redshift and D via magnitude luminosity . In fig. 13 is the measurement summarized (http://en.wikipedia.org/wiki/Hubble%27s law)

$$z = \frac{\lambda_0}{\lambda} - 1 = \sqrt{\frac{1 + v/c}{1 - v/c}} - 1$$

$$v << c \Rightarrow z \approx \frac{v}{c}$$

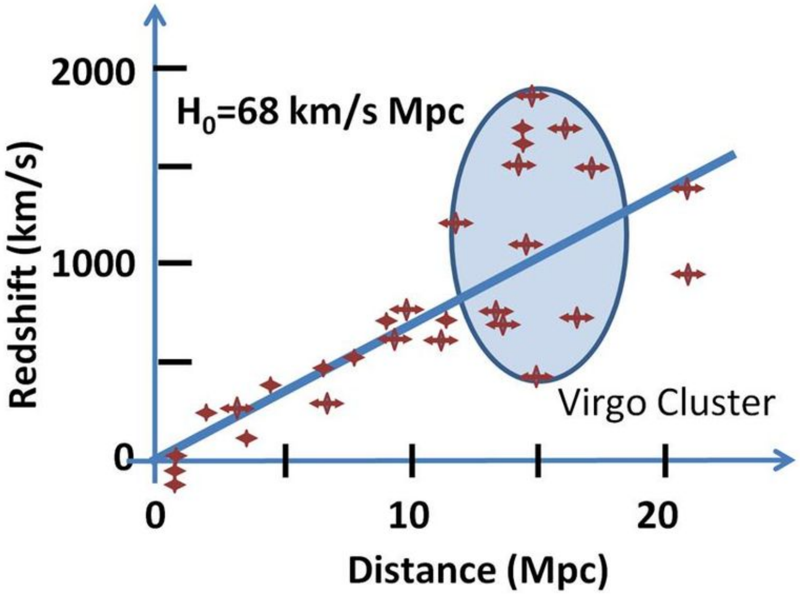

Fig. 13 Fit of redshift velocities to Hubble law after W. C. Keel (2007)
Springer pp. 7–8. ISBN 3-540-72534-2.

The HDF 3-951.2 and HDV 3-951.1 galaxies are used in the Hubble Deep Field program to investigate the parameters of the optical depth of reionization τ_{reion}. Fig. 14 shows brightness of these both galaxies (arXiv.astro-ph/9809145v1)

$$\tau_{rion} \approx \rho_e \cdot F_{HII}(z) \cdot \sigma(Thomson)$$

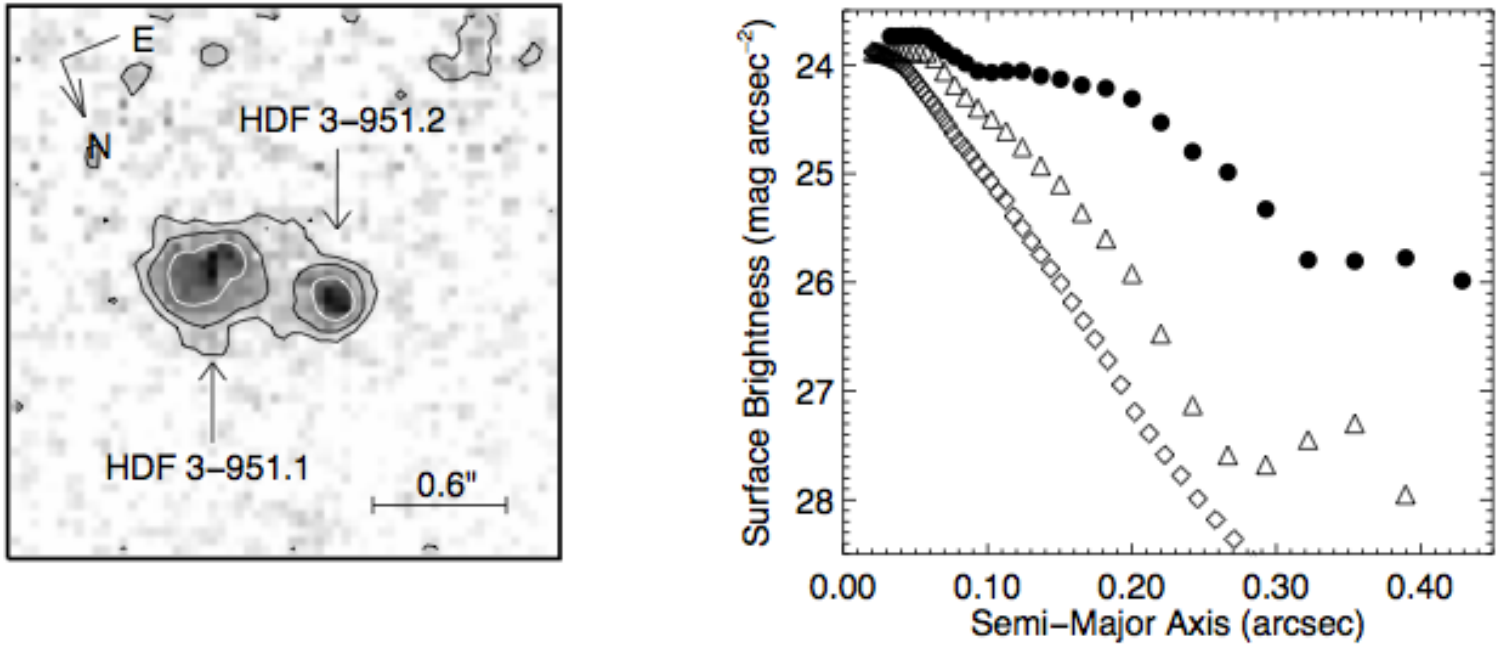

Fig. 14 Image of HDF-951.1 and HDF-3-951.2 (left) with $z = 5.34$. Surface brightness for individual components (right).

In an analysis by A. Venkatesan (The Astrophys. J. 537 (2000) 55) of an reionization model discussed in equ. 17 and constraints from CBM it was possible to get with the following parameters:

$$A(\sigma_8 = 0.7) = 1.55 \times 10^6 \quad \Omega_b = 0.05 \quad h = 0.5 \quad n = 1.0 \quad f_{esc} = 0.2 \quad f^* = 0.05 \quad \Omega_0 = 1$$

as result $\tau_{reion} = 0.0573$ with reionization occurring at $z \approx 15.5$.

Lyman-alpha forest

The Lyman-alpha forest is the sum of absorption lines arising from the Lyman-alpha transitions of the neutral hydrogen in the spectra of distance galaxies and quasars. The observations from these Lyman-alpha forest (arXiv:astro-ph/0907.2927) are also used to constrain cosmological models. These constraints agree with the WMAP data.

Structure formations

The discussed observations so far suggest that the structure formation in the universe proceeds hierarchically. First the are smallest structures followed by galaxies and then cluster of galaxies and so on like discussed before.

All these information are very crucial in constructing the Lambda-CDM model which measures the cosmological parameters, including the fraction of the Dark Energy, Dark Matter, Baryonic Matter and many other important parameters.

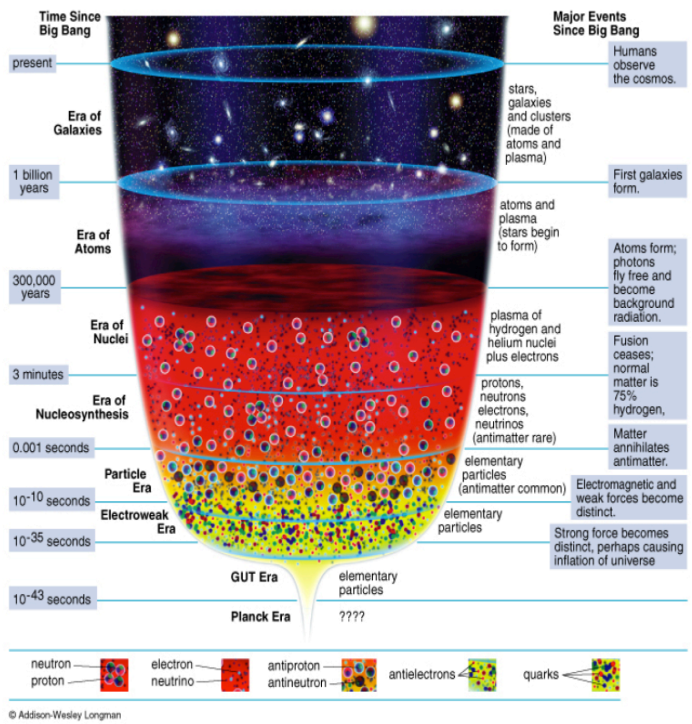

The 14 parameters of the ΛCDM model

The parameters of the ΛCDM-model (Wikipedia) are shown on the right side.

Parameter	Value	Description
t_0	$13.75 \pm 0.11 \times 10^9$ years	Age of the universe
H_0	$70.4^{+1.3}_{-1.4}$ km s^{-1} Mpc^{-1}	Hubble constant
$\Omega_b h^2$	0.02260 ± 0.00053	Physical baryon density
$\Omega_c h^2$	0.1123 ± 0.0035	Physical dark matter density
Ω_b	0.0456 ± 0.0016	Baryon density
Ω_c	0.227 ± 0.014	Dark matter density
Ω_Λ	$0.728^{+0.015}_{-0.016}$	Dark energy density
Δ_R^2	$2.441^{+0.088}_{-0.092} \times 10^{-9}$, $k_0 = 0.002 Mpc^{-1}$	Curvature fluctuation amplitude
σ_8	0.809 ± 0.024	Fluctuation amplitude at $8h^{-1}$Mpc
n_s	0.963 ± 0.012	Scalar spectral index
z_*	$1090.89^{+0.68}_{-0.69}$	Redshift at decoupling
t_*	377730^{+3205}_{-3200} years	Age at decoupling
τ	0.087 ± 0.014	Reionization optical depth
z_{reion}	10.4 ± 1.2	Redshift of reionization

These parameters are displayed in a graphic view on the next page. The parameters from this view is are taken from arXiv:astro-phy/0310723v2

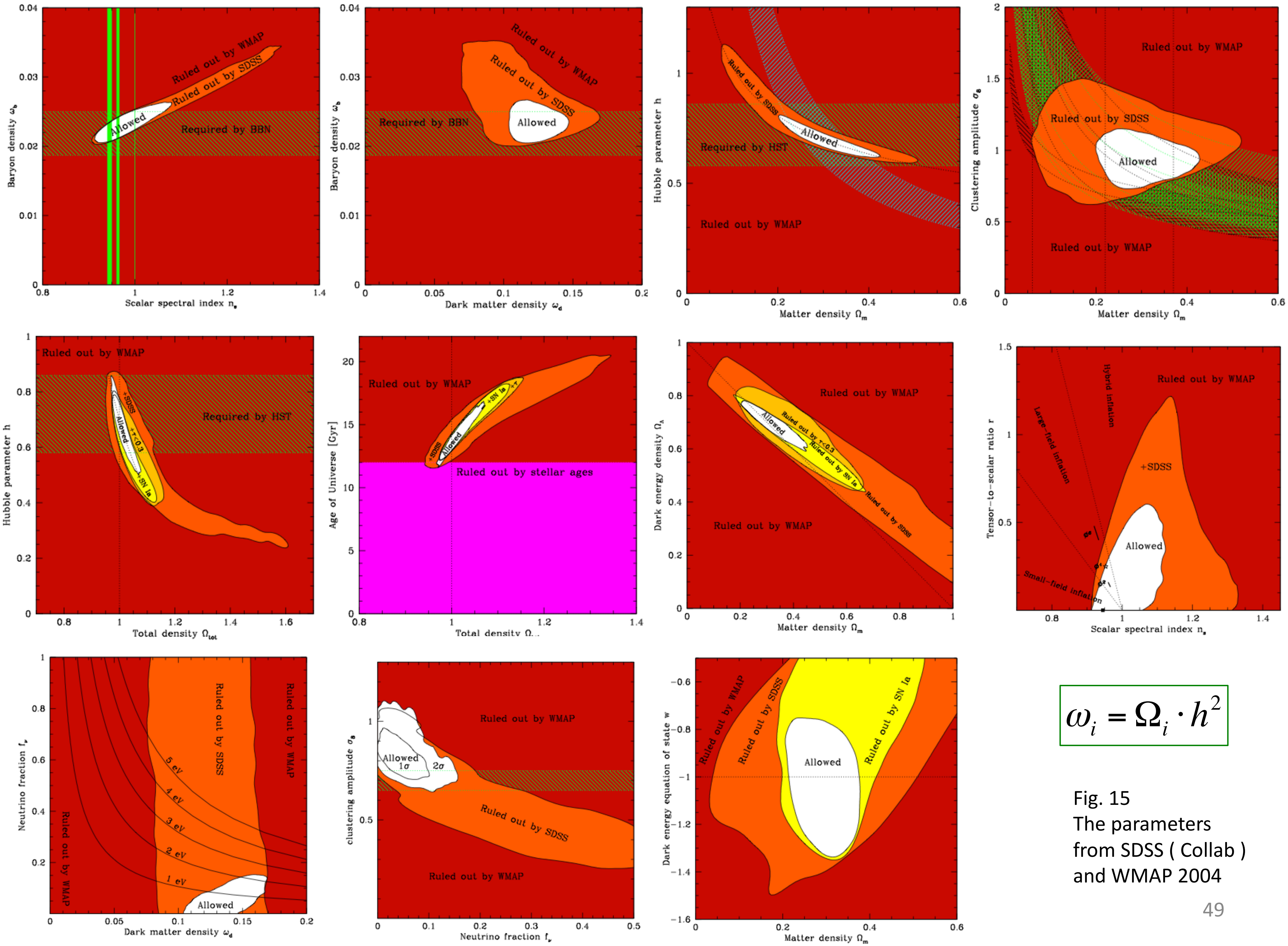

$$\omega_i = \Omega_i \cdot h^2$$

Fig. 15
The parameters from SDSS (Collab) and WMAP 2004

Experimental search for Dark Matter

The search for candidates of Dark Matter started via MACHO's, Weakly Interacting Massive Particles WIMP's, AXION's, Sterile Neutrinos, Neutralinos a. s. o.. Historically are three matter candidates are postulated:

- Cold Dark Matter is composed of heavy constituents with free-streaming length much smaller than the aria of galaxy-scale perturbations.
- Warm Dark Matter refers to particles with a free-streaming length comparable to the size of a region which evolved into a dwarf galaxy.
- Hot Dark Matter are light particles with a free-streaming length much larger than a proto-galaxy size.

Until today only the Cold Dark matter survived all considerations and searches for candidates. In particular the neutrino get ruled out, because it was not possible so far to form structures with this fast and light particles. If the dark matter has the structure of a particle the WIMP's are the most promising candidates.

The search can be divided in direct detection experiments and indirect detection experiments. A perfect overview about this field is given in " Particle Dark Matter ISBN 978-0-521-76368-4 (2010)".

Direct Detection Experiments

Direct detection is only possible in deep underground laboratories because it is absolute essential to supress the COSMIC RAY background. The laboratories are listed below:

- Soudan Mine Minnesota (US)
- Sanford Underground Research Facility (Homestake Mine) in Lead, South Dakota (US)
- SNOLAB at Sudbury Ontario (Canada)
- Grand Sasso National Laboratory (Italy)
- Canfrac Underground Laboratory (Spain)
- Modane Underground Laboratory (France)
- Boulby Underground Laboratory (UK)
- Deep underground Science and Engineering Laboratory South Dakota (US)

Detectors use in principle three detection methods. First a cryogenic technique. The detector works below 100mK and detect the heat produced when a WIMP hits an atom in a crystal absorber. Second use scintillating thallium-doped sodium iodide (Na(Tl)) crystals to measure the light with photomultipliers from recoil particles. These experiments are listed below:

- CDMS Operated by University of California, at the Soudan Mine in Minnesota (US)
- CRESST Collaboration of MPI-München, UNI-Oxford, TU-München, UNI Tübingen at Gran Sasso (Italy).
- EDELWEISS Collaboration of CNRS,CEA (France), KIT Karlsruhe (Germany), JINR Dubna (RU) Oxford UNI (UK) and Sheffield UNI (UK) at Modane (France)
- EURICA Collaboration CNRS,CEA (France), MPI-TU Münche, UNI Tübingen, KIT Karlsruhe (Germany), UNI-Zaragoza (Spain), INR (Ukraine), JINR (RU) , UNI Oxford (UK), CERN at Modana.
- DAMA DAMA/NaI and DAMA/LIBRA Collaboration of Università di Roma, INFN – Laboratori Nazionali del Gran Sasso (Italy), IHEP Beijing (China) locaded at Gran Sasso.

A third group of detectors use noble liquid gases, like liquid Xenon or Argon. If a WIMP interacts with the Xenon or Argon atoms the detectors measure the flash of scintillation light, the ionized atoms and liberated electrons in a drift technique. These experiments are listed in the following:

- ZEPLIN Collaboration, UK Dark Matter (UKDMC) (UK) , LIP-Coimbra (Portugal), ITEP-Moscow (RU) at Boulby Underground Laboratory (UK).
- XENON Big collaboration between universities and institutes in US, Switzerland, Portugal, Italy, China, Germany, France, Netherland and Israel located at Gran Sasso.
- DEAP Collaborators from Queen's University, Carleton University, Case Western Reserve University, Los Alamos National Laboratory, SNOLAB, TRIUMF, University of Alberta, University of New Mexico, University of North Carolina, and Yale University located at SNOLAB Sudbury, Ontario (Canada)
- ArDM Collaboration from CIEMAT (SP), ETH/Zurich (CH), Univ Granada (SP), Univ Sheffield (UK) , Soltan Institute Warszawa (PL) - Univ Zurich (CH) located at Canfrac Underground Laboratory (Spain).
- WARP Collaboration of INFN (University Pavia, Dell'Aquila, Napoli and Padova), Gran Sasso (INFN-LNGS) (Italy), Institute of Nuclear Physics PAN (PL) and Princeton University (US) located at Gran Sasso.
- LUX Collaboration. Brown Uni., Case Western Reserve Uni., Uni. Rochester, Lawrence Livermore Laboratory, South Dakota School of Mines and Technology, Texas A&M, UC Davis, Uni. of South Dakota, Berkeley National Lab., UC Santa Barbara, Yale Uni. (US), LIP Coimbra (Portugal) located at Homestake Mine (US)

Location of the discussed detectors

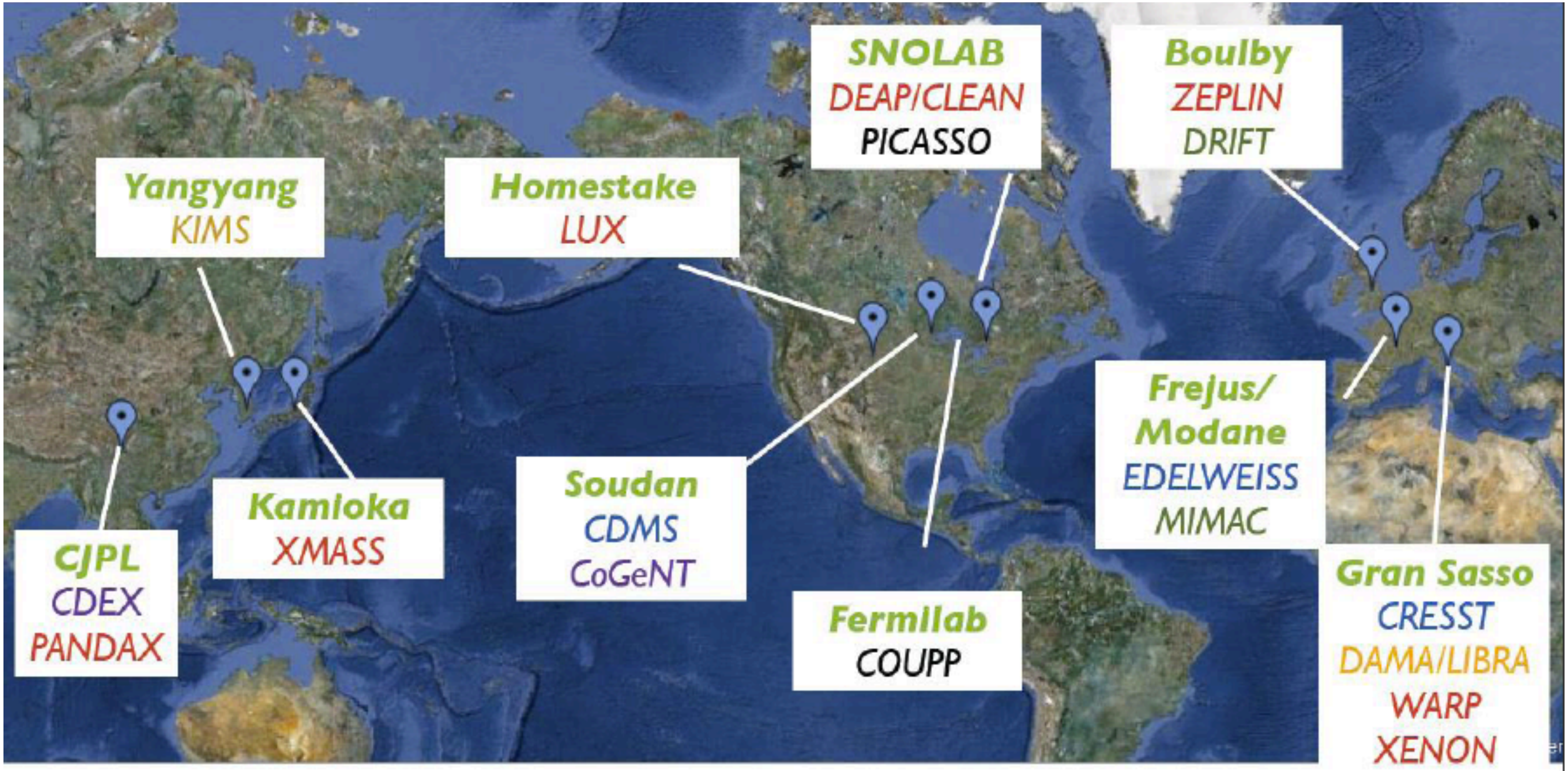

Fig. 16 World-wide distribution of the mayor direct search experiments

WIMPs Direct Detection Experiments

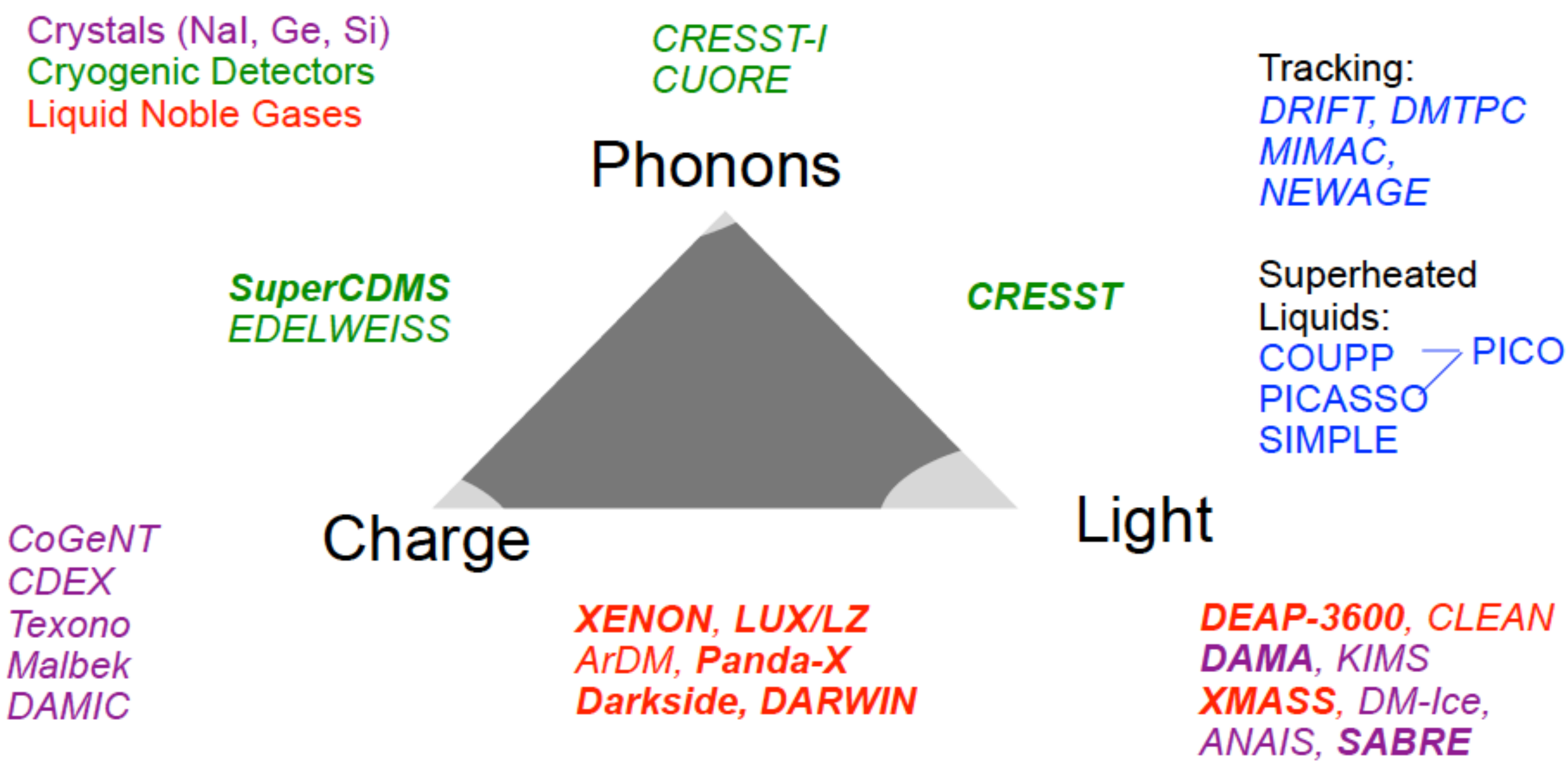

Ref. :M. Messina, Status of direct WIMP Dark Matter search, messina_now2016.pdf

Direct Dark Matter Search Experiment in China Jinping

A new deep underground experiment for direct dark matter search in on the way in Jingping and should be operational in 2015.

ref. https://wwwgerda.mpp.
mpg.de/symp/03_Yue.pdf
ref. PandaX:A dark matter experiment
in JinPing Lab

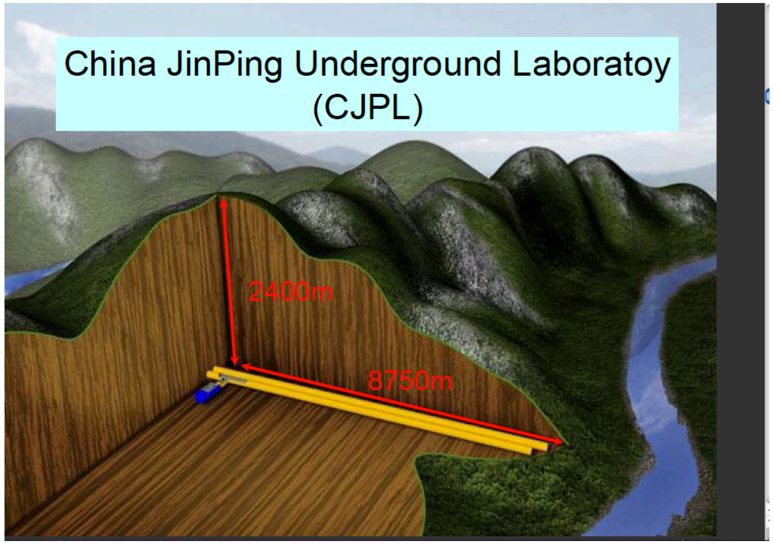

The experiment is located 2400 m under ground. The low cosmic background conditions are ideal for direct dark matter search.

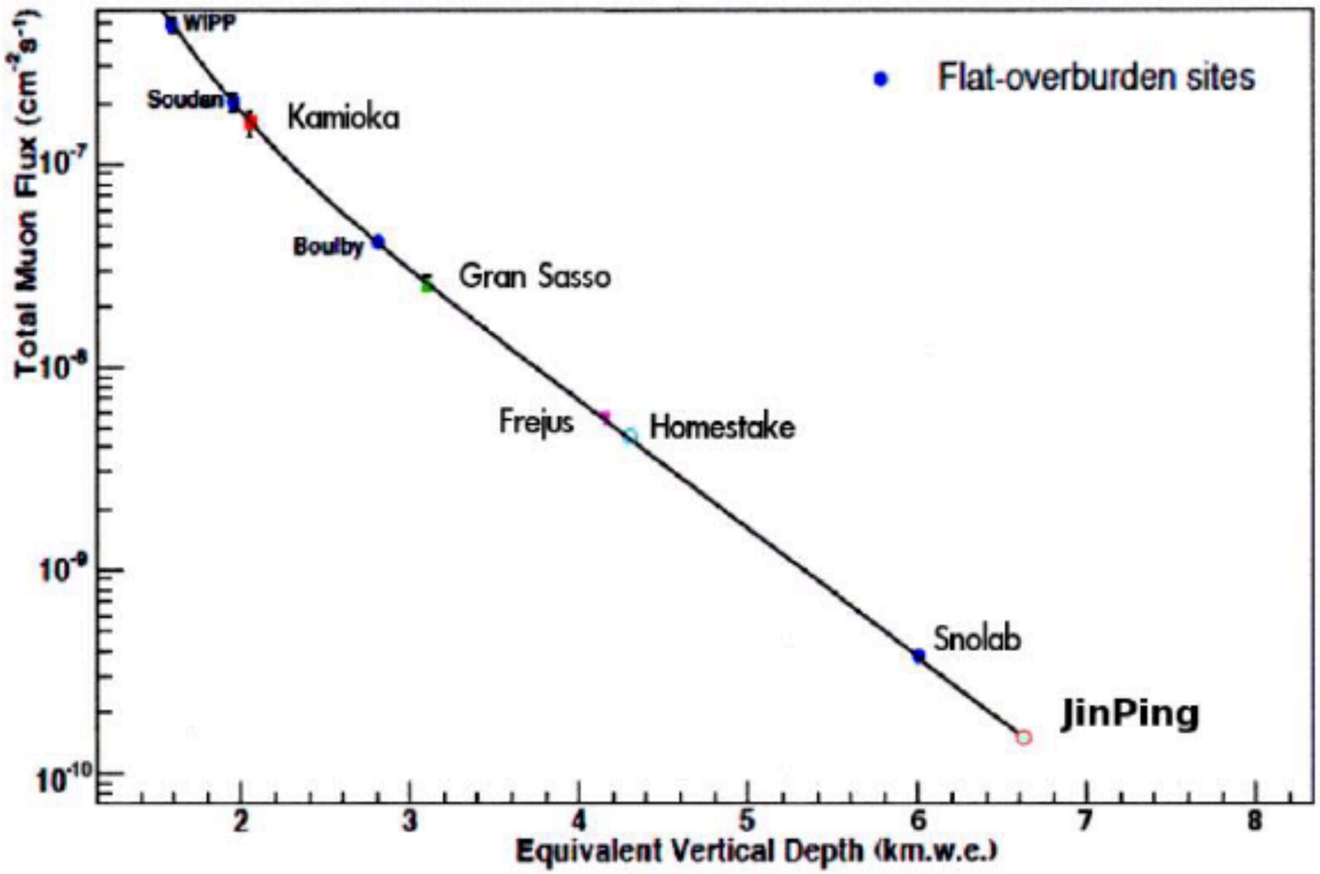

Rate modulations as SIGNAL

- The SOFT WIMP wind changes Rate and shape of nuclear recoil spectrum depend on target material, if the DM is NOT moving synchronized with the speed of the sun.
- Motion of the Earth to the galactic centre:
  - originates an event rate modulation: June - December asymmetry ~ 2-10%
  - sidereal directional modulation: asymmetry ~20-100% in forward backward event rate.

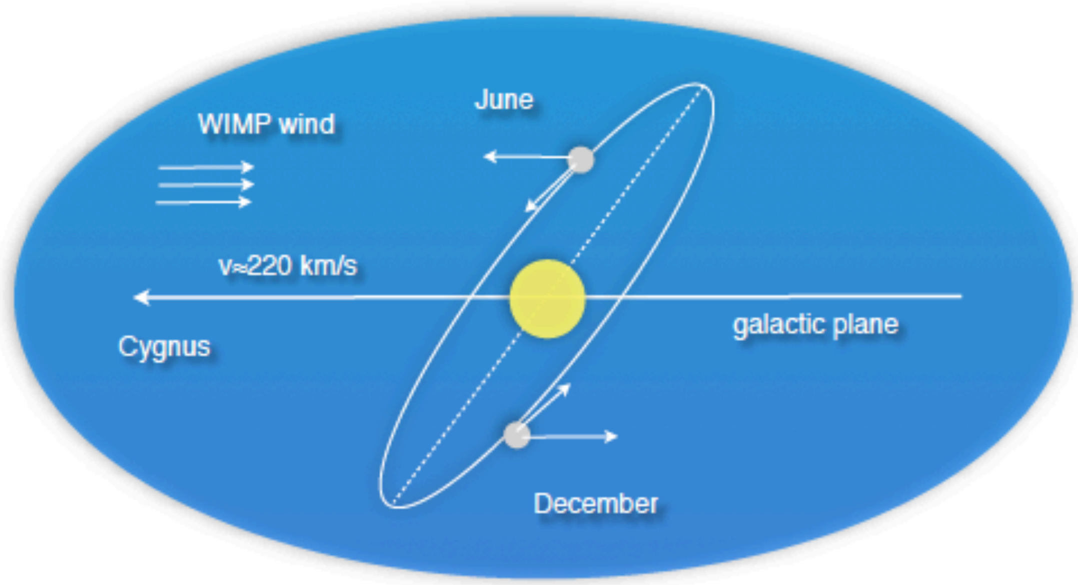

Drukier, Freese, Spergel, PRD 33,1986

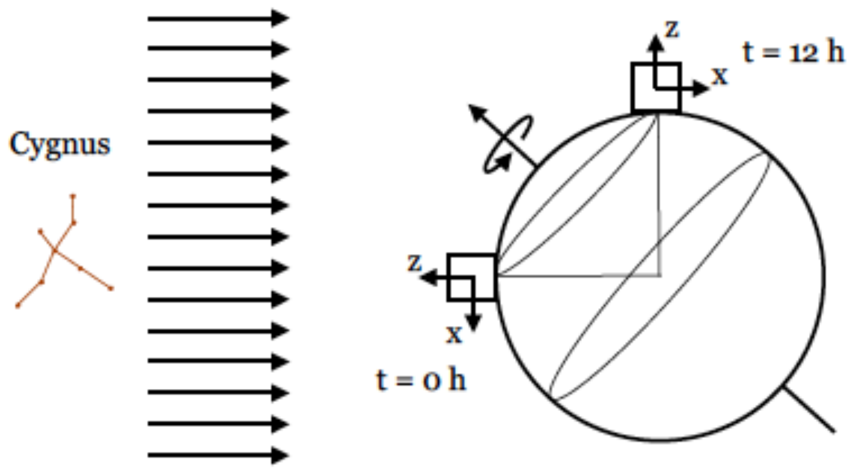

D. Spergel, PRD 36, 1988

Ref. :M. Messina, Status of direct WIMP Dark Matter search, messina_now2016.pdf

Signals are reported so far from DAMA, CDM and CRESST.

The DAMA/LIBRA detector has a target-detector mass: ~250 kg highly radiopure NaI(Tl).

The experiments measures single-hit residuals rate as function of time and energy. A clear time depending pattern is visible from fig. 17

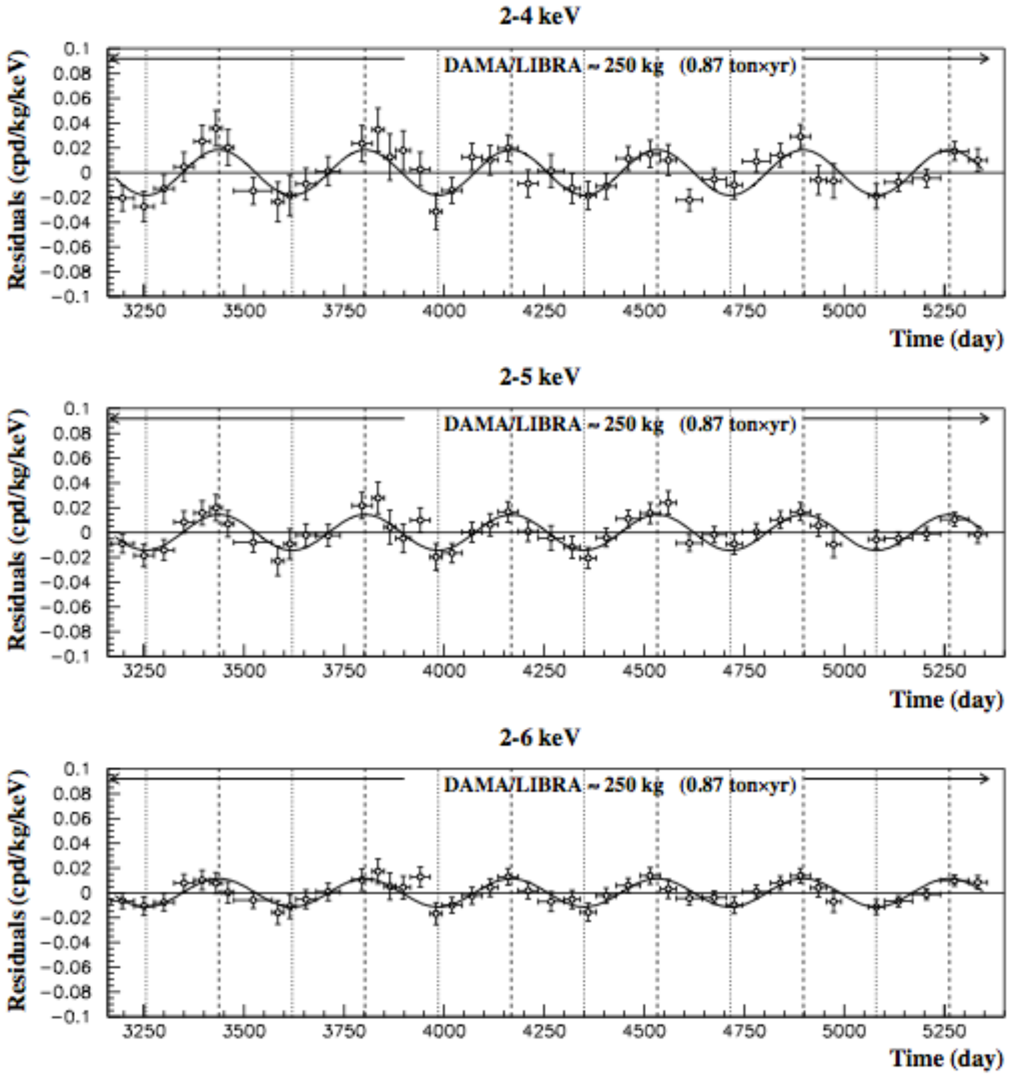

Fig. 17 Single-hit rate via measuring time.

arXiv:1002.1028v1, arXiv:astro-ph/0307403v1 2003 ;
M. Messina, Status of direct WIMP Dark Matter search,
messina_now2016.pdf

The CDM detector is a interleaved Z-sensitive ionization Phonon detector of a thin film superconducting technology. In a paper published this year (arXiv:1203.1309v1) the group measure the rate of nuclear-recoil as a function of time (blue). Assumig a nuclear-recoil energy scale, the light orange function shows a maximum–likelihood modulation in the enery range of 5.0 – 11.9 keV shown in fig. 18.

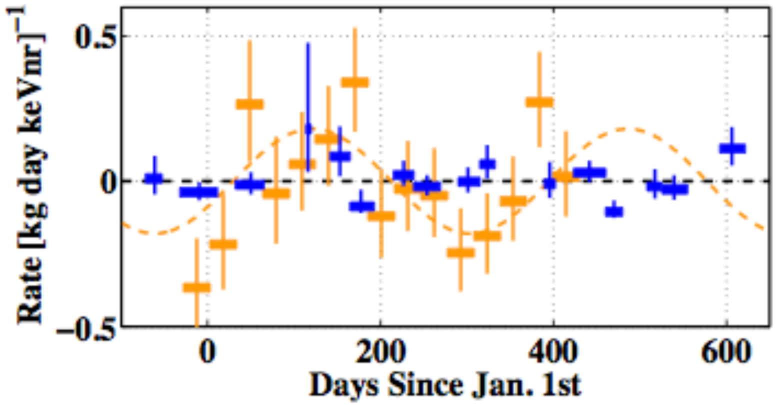

Fig. 18 The time modulation of nuclear-recoil rate.

The modulation data are still under discussion in 2014.

The CRESST group published 2011 (arXiv:1109.0702v1) sixty-seven events are found in the acceptance region where a WIMP signal in the form of low energy nuclear recoils would be expected. It was possible to contribute to a WIMP cross section mass plot shown in fig. 19.

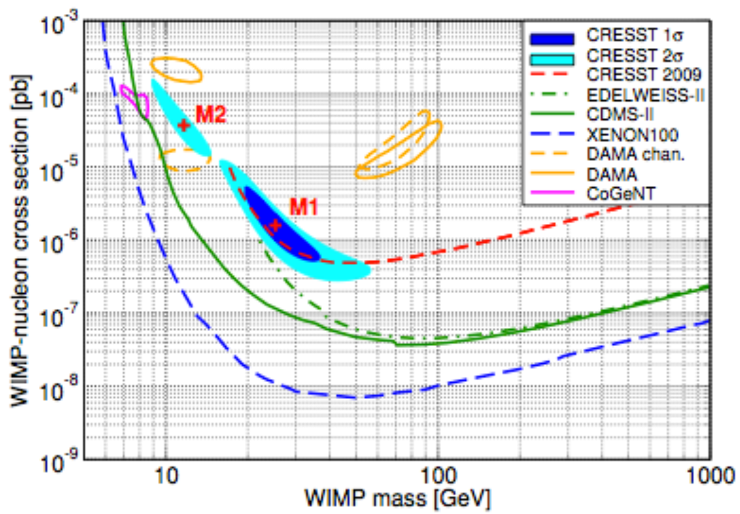

Fig. 19 WIMP σ mass plot.

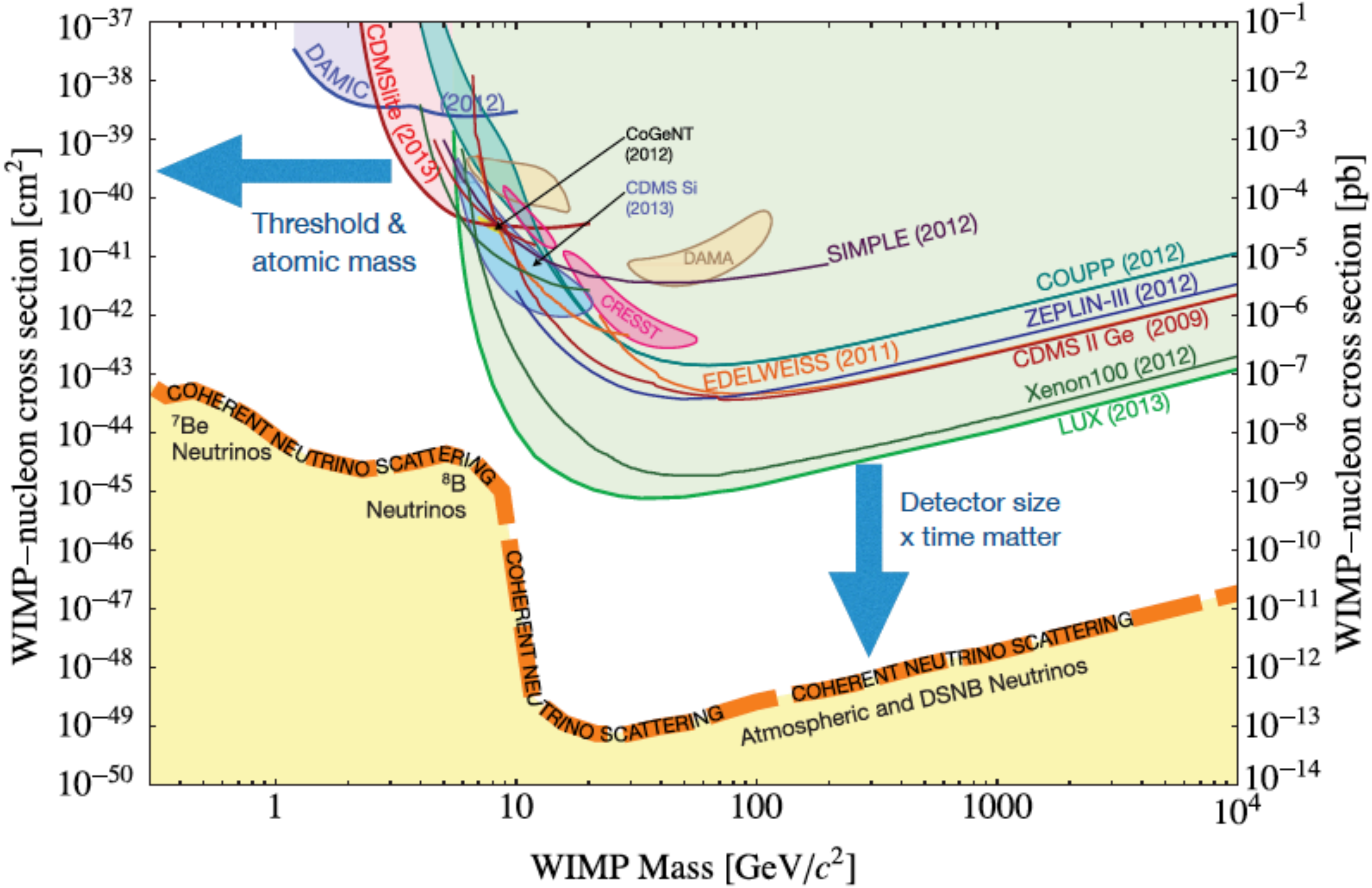

Status 2016

Ref. :M. Messina, Status of direct WIMP Dark Matter search, messina_now2016.pdf

Indirect detection experiments

Indirect detection experiments search for the products of WIMP annihilation. If WIMPs are Majorana particles then two WIMPs colliding could annihilate to produce gamma rays or particle-antiparticle pairs. This could produce a significant number of gamma rays, antiprotons or positrons in the galactic halo. An other possibility is to search for SUSY dark matter in colliders or balloon experiments like Neutralinos.

- EGRET The Energetic Gamma Ray Experiment Telescope is a Compton Gamma Ray Observatory satellite what operated from 1991 to 2000. The telescope observed more gamma rays than expected from the Milky Way.
- ATIC Observations of High Energy Cosmic Ray Electrons by the ATIC Balloon Experiment. Louisiana State Uni.(US), Marshall Space Flight Center (US), Skobeltsyn Institute of Nuclear Physics (RU), Max-Planck Inst. for Solar (GE) System Research and Purple Mountain Observatory (China) Launched 2002.
- PAMELA Is a spectrometer launched 2006. Has detected a larger number of positron than expected.
- AMS-02 A spectrometer launched 2011 is sensitive to charged particles in particular to anti-Helium, anti-Deuterium and positrons. (SUSY)
- ATLAS-CMS Both detectors at LHC searching for SUSY particles which are candidates for cold DM in particular the set limits on the mass of Neutralinos.

High Energy Cosmic Ray Electrons by the ATIC Balloon Experiment

ATIC collaboration J. Isbert (Joachim Isbert TANGO 2009)

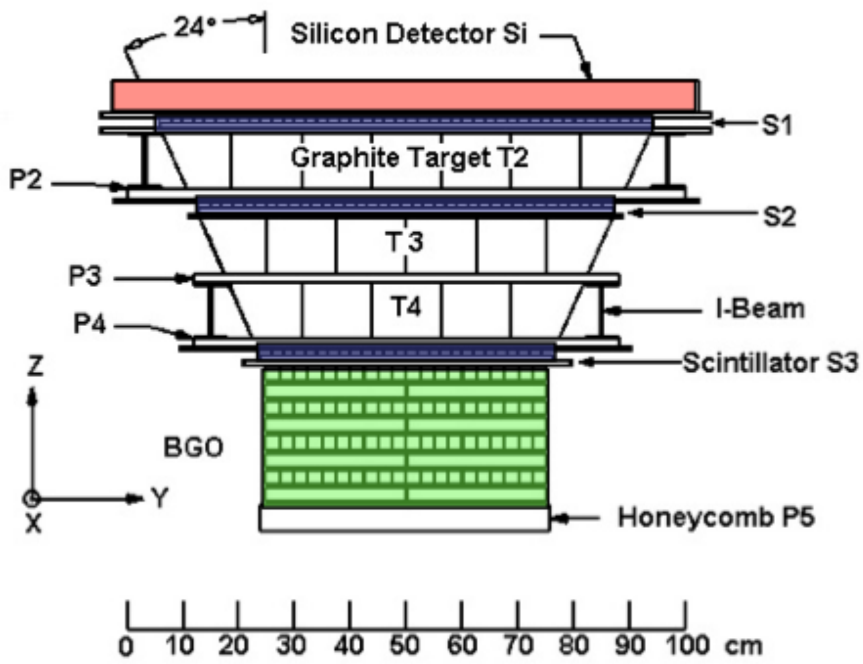

Fig. 20 The ATIC BGO electromagnetic calorimeter

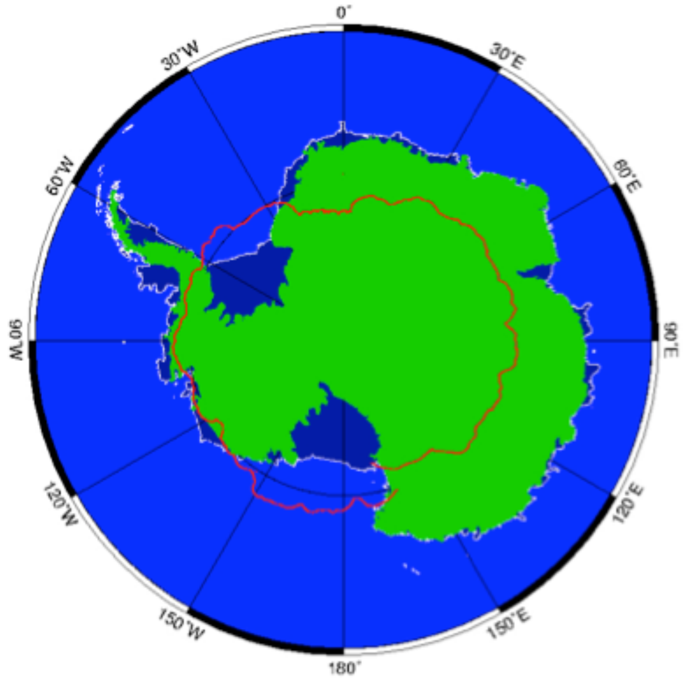

Fig. 21 The flight of ATIC at the south pole.

Launch:	12/29/02 04:59 UTC
Begin Science:	12/30/02 05:40 UTC
End Science:	01/18/03 01:32 UTC
Termination:	01/18/03 02:01 UTC
Recovery:	01/28/03; 01/30/03

The ATIC electron results

- Sum of ATIC 1 and ATIC 2 flight.
- Curves GALPROP simulation
  - Solid local interstellar space
  - dashed solar modulation
- Significance about 3.8 σ
- Emulsion chamber will be re-analyzed

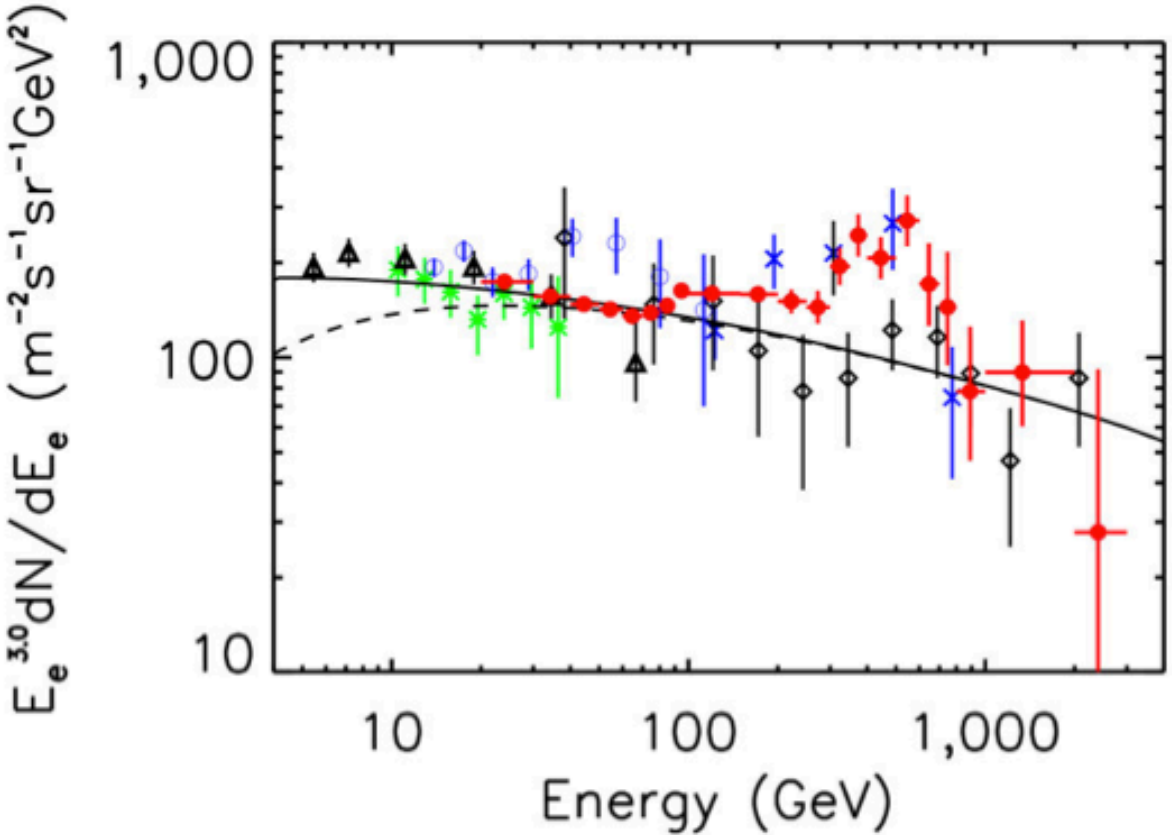

Fig 22 ● ATIC 1+2, ✱ Alpha Magnetic Spectrometer, △ HEAT magnetic spectrometer, ○ BETS, × PPB-BETS, ◇ Emulsion chambers

A WIMPs passing through the Sun or Earth they may scatter off atoms and lose energy. A large population of WIMPs could be accumulate at the center of these bodies, this would increasing the chance that the collide and annihilate. This could produce a signal in the form of high-energy neutrinos originating from the center of the Sun or Earth. Such a signal would be an indirect proof of WIMP dark matter. High-energy neutrino telescopes such as AMANDA, IceCube and ANTARES are searching for this signal.

The IceCube Neutrino Observatory at the South Pole (See fig. 23) is designed to look for point sources of neutrinos in the TeV range to explore the highest-energy astrophysical processes

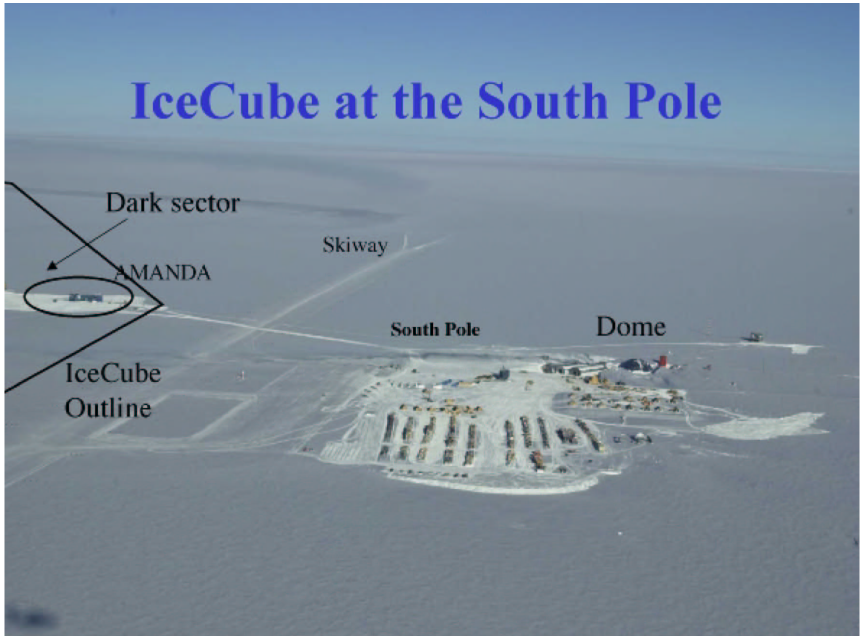

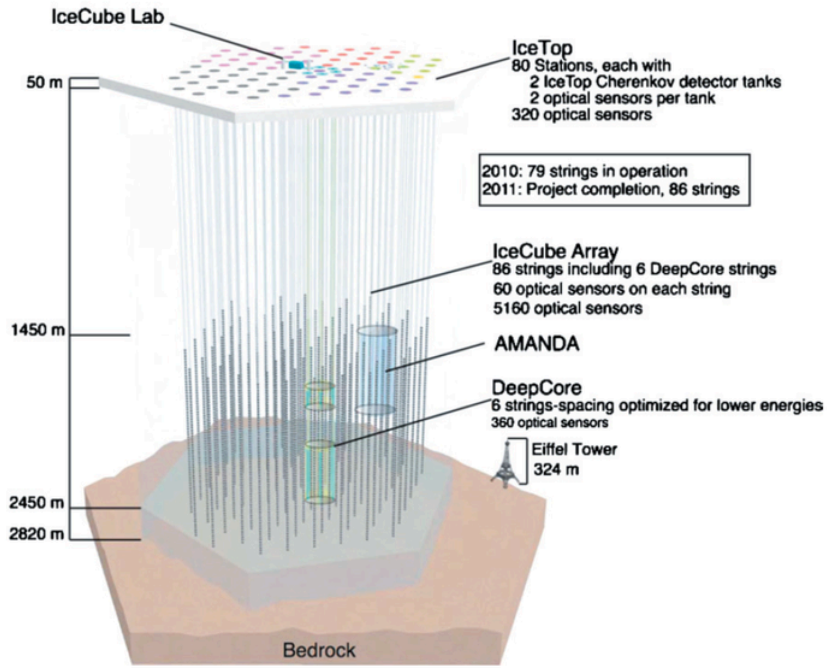

Fig. 23 The size of the IceCube detector at the South Pol (seeker401.wordpress.com)

First signals from IceCube

All Fig. and Tab. direct taken from (Science 342 1242856 (2013) and Phys.Rev.Lett.111 021103 (2013)

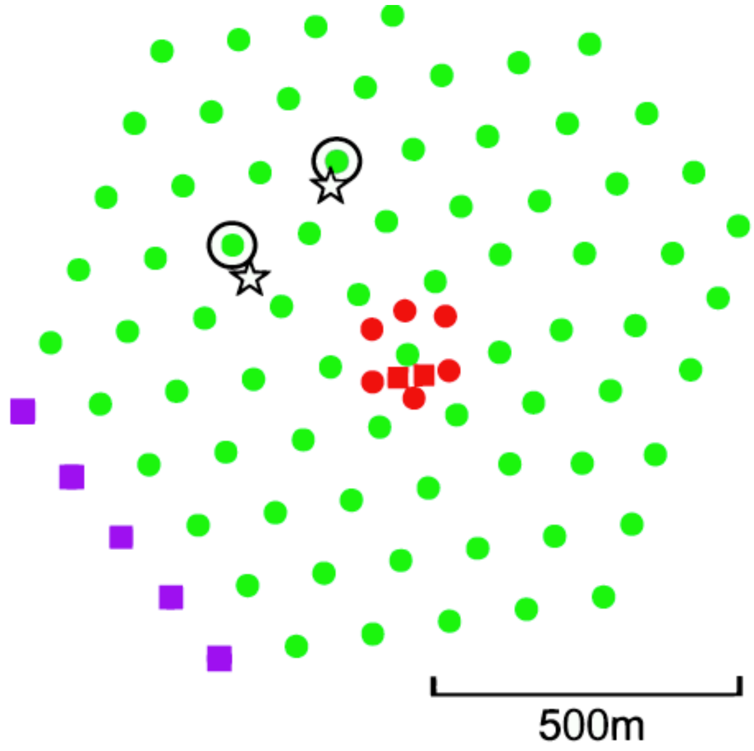

FIG. 1 (color online). Surface view of the full IceCube detector layout. Filled marks represent the positions of the IceCube strings. Red marks in the central region are the DeepCore strings. Squares represent the strings that did not exist in the IC79 configuration. Open circles are the positions of the closest strings to the observed two cascade events. Stars are their reconstructed vertex positions.

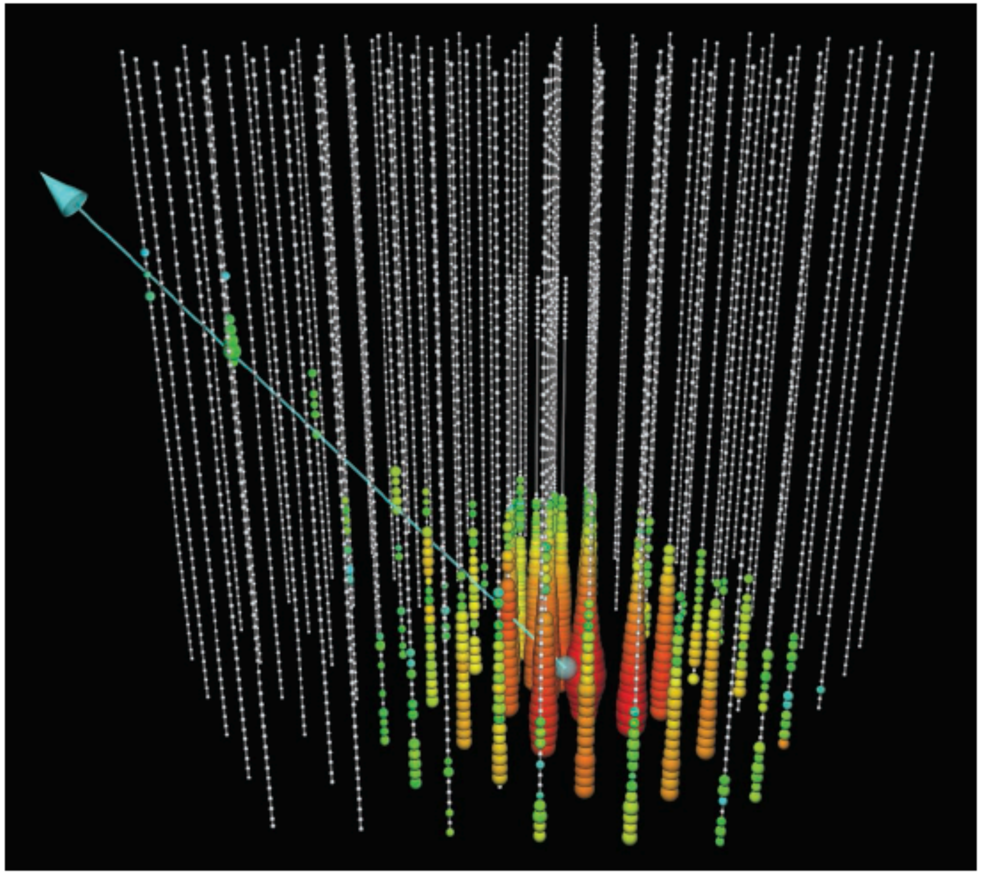

A 250 TeV neutrino interaction in IceCube. At the neutrino interaction point (bottom), a large particle shower is visible, with a muon produced in the interaction leaving up and to the left. The direction of the muon indicates the direction of the original neutrino.

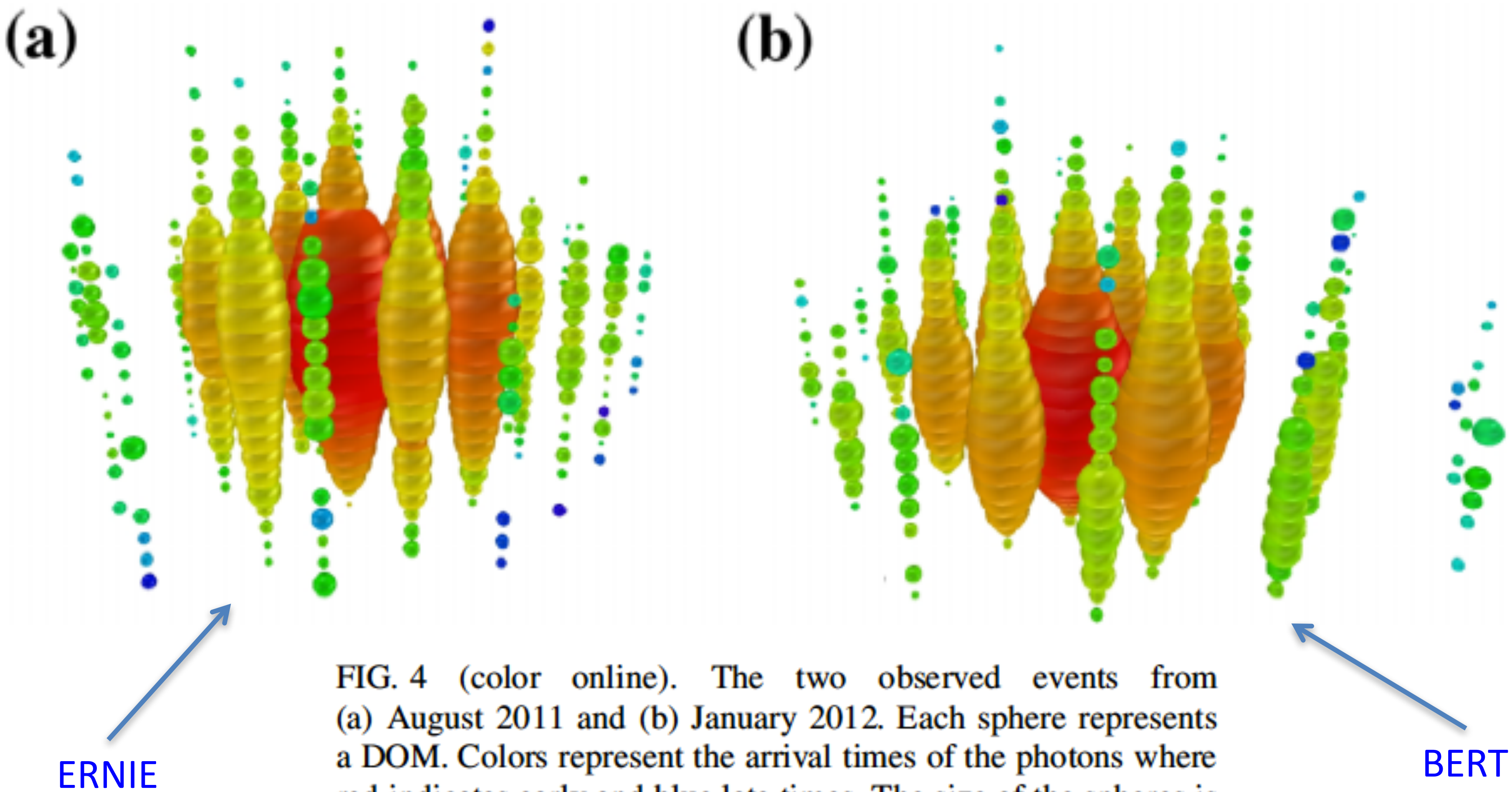

FIG. 4 (color online). The two observed events from (a) August 2011 and (b) January 2012. Each sphere represents a DOM. Colors represent the arrival times of the photons where red indicates early and blue late times. The size of the spheres is a measure for the recorded number of photoelectrons.

TABLE I. Characteristics of the two observed events. The depths of the reconstructed vertex positions "z" are with respect to the center of the IceCube detector at a depth of 1948 m.

Date (GMT)	August 8, 2011	January 3, 2012
NPE	7.0×10^4	9.6×10^4
Number of recorded DOMs	354	312
Reconstructed deposited energy (PeV)	1.04 ± 0.16	1.14 ± 0.17
Reconstructed z vertex (m)	122 ± 5	25 ± 5

In total 28 events are detected

Table 1. Properties of the 28 events. Shown are the deposited electromagnetic-equivalent energy (the energy deposited by the events in IceCube assuming all light was made in electromagnetic showers), as well as the arrival time and direction of each event and its topology (track- or showerlike). The energy shown is equal to the neutrino energy for ν_e charged-current events, within experimental uncertainties, and is otherwise a lower limit on the neutrino energy because of exiting muons or neutrinos. Errors on energy and the angle include both statistical and systematic effects. Systematic uncertainties on directions for showerlike events were determined on an individual basis; track systematic uncertainties here are equal to 1°, which is an upper limit from studies of the cosmic ray shadow of the moon (4). Additional per-event information, including event displays, can be found in the supplementary materials.

ID	Deposited energy (TeV)	Time (modified Julian date)	Declination (degrees)	Right ascension (degrees)	Median angular error (degrees)	Event type
1	$47.6^{+6.5}_{-5.4}$	55,351	−1.8	35.2	16.3	Shower
2	117^{+15}_{-15}	55,351	−28.0	282.6	25.4	Shower
3	$78.7^{+10.8}_{-8.7}$	55,451	−31.2	127.9	≤1.4	Track
4	165^{+20}_{-15}	55,477	−51.2	169.5	7.1	Shower
5	$71.4^{+9.0}_{-9.0}$	55,513	−0.4	110.6	≤1.2	Track
6	$28.4^{+2.7}_{-2.5}$	55,568	−27.2	133.9	9.8	Shower
7	$34.3^{+3.5}_{-4.3}$	55,571	−45.1	15.6	24.1	Shower
8	$32.6^{+10.3}_{-11.1}$	55,609	−21.2	182.4	≤1.3	Track
9	$63.2^{+7.1}_{-8.0}$	55,686	33.6	151.3	16.5	Shower
10	$97.2^{+10.4}_{-12.4}$	55,695	−29.4	5.0	8.1	Shower
11	$88.4^{+12.5}_{-10.7}$	55,715	−8.9	155.3	16.7	Shower
12	104^{+13}_{-13}	55,739	−52.8	296.1	9.8	Shower
13	253^{+26}_{-22}	55,756	40.3	67.9	≤1.2	Track
14	1041^{+132}_{-144}	55,783	−27.9	265.6	13.2	Shower
15	$57.5^{+8.3}_{-7.8}$	55,783	−49.7	287.3	19.7	Shower
16	$30.6^{+3.6}_{-3.5}$	55,799	−22.6	192.1	19.4	Shower
17	200^{+27}_{-27}	55,800	14.5	247.4	11.6	Shower
18	$31.5^{+4.6}_{-3.3}$	55,924	−24.8	345.6	≤1.3	Track
19	$71.5^{+7.0}_{-7.2}$	55,926	−59.7	76.9	9.7	Shower
20	1141^{+143}_{-133}	55,929	−67.2	38.3	10.7	Shower
21	$30.2^{+3.5}_{-3.3}$	55,937	−24.0	9.0	20.9	Shower
22	220^{+21}_{-24}	55,942	−22.1	293.7	12.1	Shower
23	$82.2^{+8.6}_{-8.4}$	55,950	−13.2	208.7	≤1.9	Track
24	$30.5^{+3.2}_{-2.6}$	55,951	−15.1	282.2	15.5	Shower
25	$33.5^{+4.9}_{-5.0}$	55,967	−14.5	286.0	46.3	Shower
26	210^{+29}_{-26}	55,979	22.7	143.4	11.8	Shower
27	$60.2^{+5.6}_{-5.6}$	56,009	−12.6	121.7	6.6	Shower
28	$46.1^{+5.7}_{-4.4}$	56,049	−71.5	164.8	≤1.3	Track

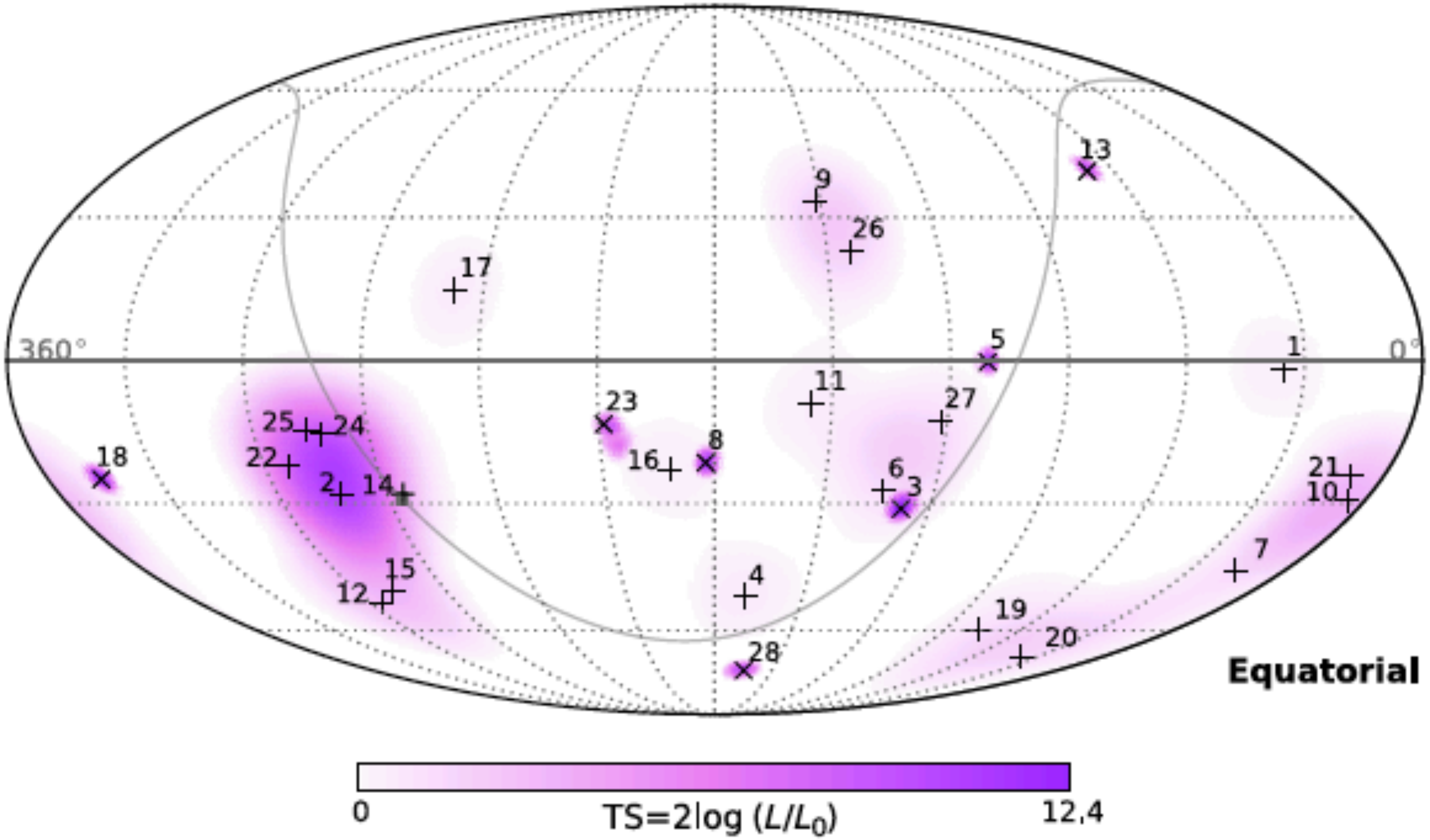

Fig. 5. Sky map in equatorial coordinates of the TS value from the maximum likelihood point source analysis. The most significant cluster consists of five events—all showers and including the second highest energy event in the sample—with a final significance of 8%. This is not sufficient to identify any neutrino sources from the clustering study. The galactic plane is shown as a curved gray line with the galactic center at the bottom left denoted by a filled gray square. Best-fit locations of individual events (listed in Table 1) are indicated with vertical crosses (+) for showers and angled crosses (×) for muon tracks.

(Statistic values TS, L is the maximized likelihood and L_0 null hypothesis)

CONCLUSION

The Einstein equations as source of the Big Bang theory and the ΛCDM model together with extensive observations in the last 100 years have established high evidence of DARK MATTER.

To understand the nature of DARK MATTER is an important exciting problem of the future.